Stony Brook University

Dynamic Heat Transfer: Effective Heat Capacity of Planar Thermal Mass Subject to Periodic Heating and Cooling

A Thesis Presented

by

Peizheng Ma

to

The Graduate School

in Partial Fulfillment of the

Requirements

for the Degree of

Master of Science

in

Mechanical Engineering

Stony Brook University

May 2010

Stony Brook University

The Graduate School

Peizheng Ma

We, the thesis committee for the above candidate for the

Master of Science degree, hereby recommend

acceptance of this thesis.

Lin-Shu Wang – Thesis Advisor
Associate Professor, Department of Mechanical Engineering

Jon Longtin - Chairperson of Defense
Associate Professor, Department of Mechanical Engineering

John M. Kincaid
Professor, Department of Mechanical Engineering

This thesis is accepted by the Graduate School

Lawrence Martin
Dean of the Graduate School

Abstract of the Thesis

Dynamic Heat Transfer: Effective Heat Capacity of Planar Thermal Mass Subject to Periodic Heating and Cooling

by

Peizheng Ma

Master of Science

in

Mechanical Engineering

Stony Brook University

2010

The design-application of thermal mass is a powerful tool for controlling temperature in buildings. Although a large volume of literature on the use of thermal masses in building applications exists, little quantitative characterization of the performance of a thermal mass under dynamic heating and cooling can be found. In this thesis, the performance of planar thermal masses (PTMs) subject to sinusoidal heating and cooling is investigated.

Based on the analysis of a semi-infinite PTM under a sinusoidal thermal wave, some new definitions — penetration depth, effective thickness, effective area specific heat and effective heat exchange coefficient are introduced.

Since actual PTMs are not semi-infinite, the dynamic heat transfer process of finite-thickness PTMs — one surface is under a sinusoidal thermal wave and the other

one is specified with three kinds of boundary conditions— are discussed.

When inside air temperature is equal to the mean value of the outside surface temperature, analytical solutions of the temperature distribution and heat flux in finite-thickness PTMs are deduced. The effective heat exchange coefficient and, a new definition, the effective heat storage coefficient of PTMs with different thermo-physical properties are developed. For PTMs with the boundary condition of the second kind, an optimal effective thermal mass coefficient at an optimal thermal mass thickness is found. Because of the large effective area specific heat difference, wood is much worse than concrete for heat storage.

When the inside air temperature is not equal to the mean value of the outside surface temperature, analytical solutions do not exist and numerical method is used to solve the dynamic heat transfer problem. Three forms of approximated temperature distribution are developed based on numerical calculations. The best one of the approximated forms is used to investigate the heat exchange between finite-thickness PTMs and the environment. From the approximated form, time lag and decrement factor are also obtained. Last, the comparison of wood and concrete, as exterior wall material, shows that wood is a better than concrete due to its lower conductivity.

Keywords: Dynamic heat transfer; Planar thermal mass (PTM); Heat capacity; Heat exchange; Heat storage; Periodic heating and cooling

Table of Contents

List of Figures

List of Tables

Acknowledgements

I would like to express my deepest gratitude to my thesis advisor—Professor Lin-Shu Wang, who gave me the chance to study in Stony Brook University and do the research on building energy dynamics under his guidance. I thank him for his help, motivation and encouragement in learning, as well as in everyday life. His creative passion and broad knowledge are priceless to my research and will benefit me greatly in the future.

Many thanks to the other members of my thesis committee—Professor Jon Longtin and Professor John M. Kincaid, who reviewed my work in such a short time and gave me many useful suggestions.

I am very grateful to the faculty and staff of the department of Mechanical Engineering, especially Diane, for their suggestions, help and support.

I thank the department of Mechanical Engineering and Stony Brook University for giving me the opportunity and financial support to study and research in such a beautiful and lifeful campus.

I would like to express my sincere gratitude for all of my friends, both in China and the United States. When life is tough, their friendship, kindness and support always come in time to help me conquer difficulties.

I am also thankful to my relatives for their familial affection and support.

Most of all, I would like to thank my beloved family, to whom I dedicate this work, for their forever love. The selfless sacrifice and support of my parents is always the motivity of my progress. The constant love, understanding and encouragement of my wife, Nianhua Guo, make the experience of studying abroad easier, more pleasure and more precious. Last but not the least, special thanks to my newborn son, for the happiness, as well as troubles, he given.

Chapter 1: Introduction

1.1 Background and motivation

A **thermal mass** [1~3], which can be in the form of water, earth, rock, wood, brick, or concrete, has the ability to absorb and store heat energy during a warm time (acts as a heat sink) and to release it at a cool time later (acts as a heat source). The design-application of thermal mass is a powerful tool for controlling temperature and "appropriate use of thermal mass throughout your home can make a big difference to comfort and heating and cooling bills." ([1]: page 114) There exists a large volume of architectural literature on the use of thermal masses in building applications. [1~33] However, little quantitative characterization of the performance of a thermal mass that go beyond intuitive rule-of-thumb can be found in these literatures.

Two common measures of the performance of a thermal mass are heat capacity per unit mass (i.e., **mass specific heat** c_p [kJ/kg·K]), and heat capacity per unit volume (i.e., **volumetric specific heat** c_{vol} [kJ/m^3·K], which is the product of the density ρ [kg/m^3] and the mass specific heat c_p). If a thermal mass system is subject to a *quasi-static* heating or cooling, the energy balance equation of the system is:

$$Q = mc_p\Delta T = \rho Vc_p\Delta T = Vc_{vol}\Delta T = ALc_{vol}\Delta T \qquad (1.1)$$

where Q [kJ] is the amount of heat energy put into or flowed out of a thermal mass, m [kg] is the mass, V [m^3] is the volume, and ΔT [K or °C] is the change in temperature. (A and

L—see the following)

A typical building thermal mass is a planar layer of a given thickness *L* [m] and such thermal mass can be called Planar Thermal Mass (PTM). In buildings, therefore, we are more interested in the heat capacity per unit surface area *A* [m^2] ($Q/(A\Delta T)$, i.e., the **area specific heat** c_{area} [$kJ/m^2 \cdot K$]) of a building planar material at a given thickness *L*. The c_{area} of such mass would equal to the product of c_{vol} and *L*, if it is subject to quasi-static heating or cooling. However, a building thermal mass system/unit — especially ones that is in direct interaction with ambient surroundings — is subject to a *dynamic* (time-dependent) heating or cooling, rather than a quasi-static ones. In such a situation, Eqn. (1. 1) fails to explain why a wood wall of twice or three-times, even four-times the thickness of a concrete wall (considering that the volumetric specific heat of wood and concrete are about 705 and 1844 $kJ/m^3 \cdot K$, respectively) is still a much poorer thermal mass than the concrete wall.

Therefore, it is necessary to approach this problem of building thermal mass as a dynamic problem. If weather conditions are very similar for several days, the diurnal temperature variations can be considered approximately as a sine wave; the outside surface temperature of the building envelope (usually includes walls, roof and ceiling, and floor, which can all be treated as PTMs) may be regarded approximately as a sinusoidal function with a period of 24 hours (because of the convective effect at the outside surface, the surface temperature is not equal to the outdoor air temperature; later, the effect will be considered and temperatures will be modified). The dynamic heat

transfer problem of PTMs can then be idealized in terms of periodic heating and cooling of a diurnal period P [s]. In this thesis, the **effective heat capacity** of planar PTMs under a **sinusoidal thermal wave** — will be investigated.

1.2 Thesis structure

In Chapter 2, the dynamic heat transfer of a semi-infinite PTM will be investigated. The temperature distribution and the heat flux in the PTM and the net heat exchange between the PTM and the environment will be deduced. The definitions of effective thickness, the effective area specific heat and the effective heat exchange coefficient will be introduced.

In Chapter 3, when the inside air temperature is equal to the mean value of the outside surface temperature, the dynamic heat transfer of finite-thickness PTMs under three kinds of boundary conditions will be investigated. The temperature distribution in the PTMs will be deduced. The heat exchange between the PTMs and the environment (the effective heat exchange coefficient and the inner effective heat exchange coefficient) and the heat storage of the PTMs (the effective heat storage coefficient) will be developed. The time when the outside surface heat flux is equal to zero and the time when the amount of heat stored in or released out of the PTMs is maximum will also be obtained. Two examples (the comparison of wood and concrete wall; internal PTMs) will be given at the end of the chapter. More new definitions — the dimensionless thickness, the dynamic Biot number, the optimal thermal mass thickness, the optimal effective thermal

mass coefficient, the optimal dimensionless thickness, the effective thermal resistance and the dimensionless heat flux — will be introduced in Chapter 3.

In Chapter 4, when the inside air temperature is not equal to the mean value of the outside surface temperature, the dynamic heat transfer of finite-thickness PTMs will be investigated. Since analytical solutions do not exist under this condition, the finite-difference method, one of the most frequently used numerical methods, will be used to solve the problem. Later, based on numerical calculation results, approximated temperature distribution forms will be developed. Then one of the approximated forms will be used to obtain the coefficients of wood and concrete walls, the time-lag effect and the decrement factor.

In Chapter 5, several main conclusions will be summarized and some suggestions for future work will be given.

Chapter 2: Dynamic Heat Transfer of a Semi-infinite PTM

2.1 Problem description

Consider the semi-infinite PTM shown in Figure 2.1. The left surface temperature T_0 of the PTM is a sinusoidal function with a mean value T_m. The peak amplitude and the period of T_0 are $(\Delta T)_0$ and P, respectively. Under the influence of the thermal wave at the surface, the near-surface temperature of the PTM will change continuously. However, after a certain depth, the far interior temperature will *almost* not be affected by the surface thermal wave. We can take the temperature at far interior to be *nearly* a constant T_{in} (assumed to be equal to T_m). This certain depth is called **penetration depth $\boldsymbol{L_{pene}}$** [m] (See [34]: page 320, the definition of penetration depth for the case of a step surface temperature variation; in this thesis, we will give another definition of penetration depth for the case of a sinusoidal surface temperature variation.). Suppose that all the thermo-physical properties of the PTM (i.e., ρ, c_p, c_{vol}, conductivity k [W/m·K], and thermal diffusivity α [m^2/s]) to be constants. This problem can be dealt with as a one-dimensional (x direction) heat transfer problem. The temperature changes in the PTM will repeat themselves periodically if the surface temperature variations have occurred for a sufficiently long period of time.

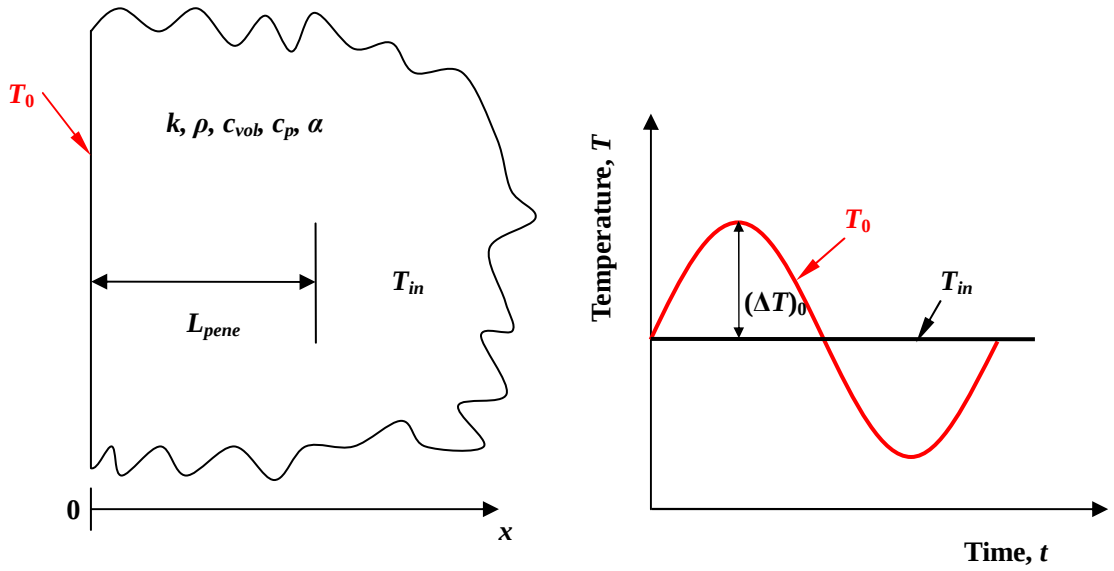

Figure 2.1—Semi-infinite PTM and its surface and far interior temperatures

Since T_0 is not constant, it is not a steady-state but a *dynamic* heat conduction problem (In reference [34], it is also referred to as *quasi-steady* conduction, which "is meant that the unsteady temperature changes repeat themselves steadily". Note: it is NOT *quasi-static* conduction). In the absence of internal energy sources/sinks, the **heat diffusion equation** should be used to calculate the temperature distribution in the PTM:

G.D.E.: $$\frac{\partial^2 T}{\partial x^2} = \frac{1}{\alpha}\frac{\partial T}{\partial t} \tag{2. 1}$$

Boundary Conditions (B.C.s) of the Governing Differential Equation (G.D.E) are:

B.C.s: $$T\left(x \to \infty, t\right) = T_{in} \tag{2. 2}$$

$$T\left(0, t\right) = T_0 = \left(\Delta T\right)_0 \sin\left(\frac{2\pi}{P} t\right) + T_m \tag{2. 3}$$

2.2 Mathematical deduction of the problem

In reference [34]: page 213~218, a smart method was given to solve the heat transfer problem just described in last section.

By defining a temperature variable as

$$\theta(x,t) = T(x,t) - T_m \tag{2. 4}$$

the G.D.E. and B.C.s can be rewritten as

G.D.E.: $$\frac{\partial^2 \theta}{\partial x^2} = \frac{1}{\alpha}\frac{\partial \theta}{\partial t} \tag{2. 5}$$

B.C.s: $$\theta(x \to \infty, t) = T_{in} - T_m = 0 \tag{2. 6}$$

$$\theta(0,t) = T_0 - T_m = (\Delta T)_0 \sin\left(\frac{2\pi}{P}t\right) \tag{2. 7}$$

Then introduce an auxiliary problem with the G.D.E. and B.C.s:

G.D.E.: $$\frac{\partial^2 \theta_0}{\partial x^2} = \frac{1}{\alpha}\frac{\partial \theta_0}{\partial t} \tag{2. 8}$$

B.C.s: $$\theta_0(x \to \infty, t) = 0 \tag{2. 9}$$

$$\theta_0(0,t) = (\Delta T)_0 \cos\left(\frac{2\pi}{P}t\right) \tag{2. 10}$$

Define a (complex) temperature function as:

$$\theta_c(x,t) = \theta_0(x,t) + i\theta(x,t) \tag{2. 11}$$

where $i = \sqrt{-1}$. The complex function $\theta_c(x,t)$ satisfies the following differential equation and B.C.s:

D.E.: $$\frac{\partial^2 \theta_c}{\partial x^2} = \frac{1}{\alpha}\frac{\partial \theta_c}{\partial t} \tag{2. 12}$$

B.C.s: $\theta_c\left(x\to\infty,t\right)=0$ (2. 13)

$$\theta_c\left(0,t\right)=\left(\Delta T\right)_0 e^{\frac{2i\pi}{P}t} \tag{2. 14}$$

Assume a product solution in the form

$$\theta_c\left(x,t\right)=X\left(x\right)e^{\frac{2i\pi}{P}t} \tag{2. 15}$$

and substitute it into Eqn. (2. 12) and get:

$$\frac{d^2X}{dx^2}-\frac{2i\pi}{\alpha P}X\left(x\right)=0 \tag{2. 16}$$

The solution of Eqn. (2. 16) can be written as

$$X\left(x\right)=C_1e^{\sqrt{\frac{2i\pi}{\alpha P}}x}+C_2e^{-\sqrt{\frac{2i\pi}{\alpha P}}x} \tag{2. 17}$$

where C_1 and C_2 are constant. Combine Eqn. (2. 15) and Eqn. (2. 17), and the application of the B.C.s (2. 13) and (2. 14) yields $C_1=0$ and $C_2=\left(\Delta T\right)_0$. Therefore,

$$\theta_c\left(x,t\right)=\left(\Delta T\right)_0 e^{-\sqrt{\frac{2i\pi}{\alpha P}}x}e^{\frac{2i\pi t}{P}}=\left(\Delta T\right)_0 e^{-(1+i)\sqrt{\frac{\pi}{\alpha P}}x}e^{\frac{2i\pi t}{P}}=\left(\Delta T\right)_0 e^{-\sqrt{\frac{\pi}{\alpha P}}x}e^{i\left(\frac{2\pi}{P}t-\sqrt{\frac{\pi}{\alpha P}}x\right)}$$

$$\Rightarrow\theta_c\left(x,t\right)=\left(\Delta T\right)_0 e^{-\sqrt{\frac{\pi}{\alpha P}}x}\left[\cos\left(\frac{2\pi}{P}t-\sqrt{\frac{\pi}{\alpha P}}x\right)+i\sin\left(\frac{2\pi}{P}t-\sqrt{\frac{\pi}{\alpha P}}x\right)\right] \tag{2. 18}$$

Finally, from the definition (2. 11), the temperature variation can be obtained as

$$\theta\left(x,t\right)=\left(\Delta T\right)_0 e^{-\sqrt{\frac{\pi}{\alpha P}}x}\sin\left(\frac{2\pi}{P}t-\sqrt{\frac{\pi}{\alpha P}}x\right) \tag{2. 19}$$

Comparing Eqn. (2. 19) with Eqn (2. 7), it is clear that the period of the temperature variation in the PTM is the same as the period of T_0, but lags by a phase difference:

$$\Delta t=\frac{x}{2}\sqrt{\frac{P}{\pi\alpha}} \tag{2. 20}$$

and the amplitude decreases exponentially with the distance x:

$$(\Delta T)_x = (\Delta T)_0 e^{-\sqrt{\frac{\pi}{\alpha P}}x} \tag{2. 21}$$

and the wavelength is:

$$x_0 = 2\sqrt{\pi\alpha P} \tag{2. 22}$$

2.3 Further discussions

Here we define the penetration depth L_{pene} as

$$L_{pene} \equiv \sqrt{2\pi\alpha P} \tag{2. 23}$$

In fact, the proportion of the amplitude at $x = L_{pene} = \sqrt{2\pi\alpha P}$ to that of T_0 is:

$$\frac{(\Delta T)_{L_{pene}}}{(\Delta T)_0} = e^{-\sqrt{\frac{\pi}{\alpha P}}\sqrt{2\pi\alpha P}} = e^{-\sqrt{2}\pi} \approx 0.0118 = 1.18\% \tag{2. 24}$$

which means that the amplitude $(\Delta T)_0$ decreases 98.82% at $x = L_{pene}$.

With the definition of the penetration depth, Eqn. (2. 19) can be rewritten as

$$\theta(x,t) = (\Delta T)_0 e^{-\frac{\sqrt{2}\pi x}{L_{pene}}} \sin\left(\frac{2\pi t}{P} - \frac{\sqrt{2}\pi x}{L_{pene}}\right) \tag{2. 25}$$

Hour by hour temperature distribution for a PTM with a thickness of $L = 2L_{pene}$ is shown in Figure 2.2. Note: the temperature distribution of a $2L_{pene}$-thick PTM is good enough to represent that of a semi-infinite PTM since $e^{-2\sqrt{2}\pi} \approx 0.00014$.

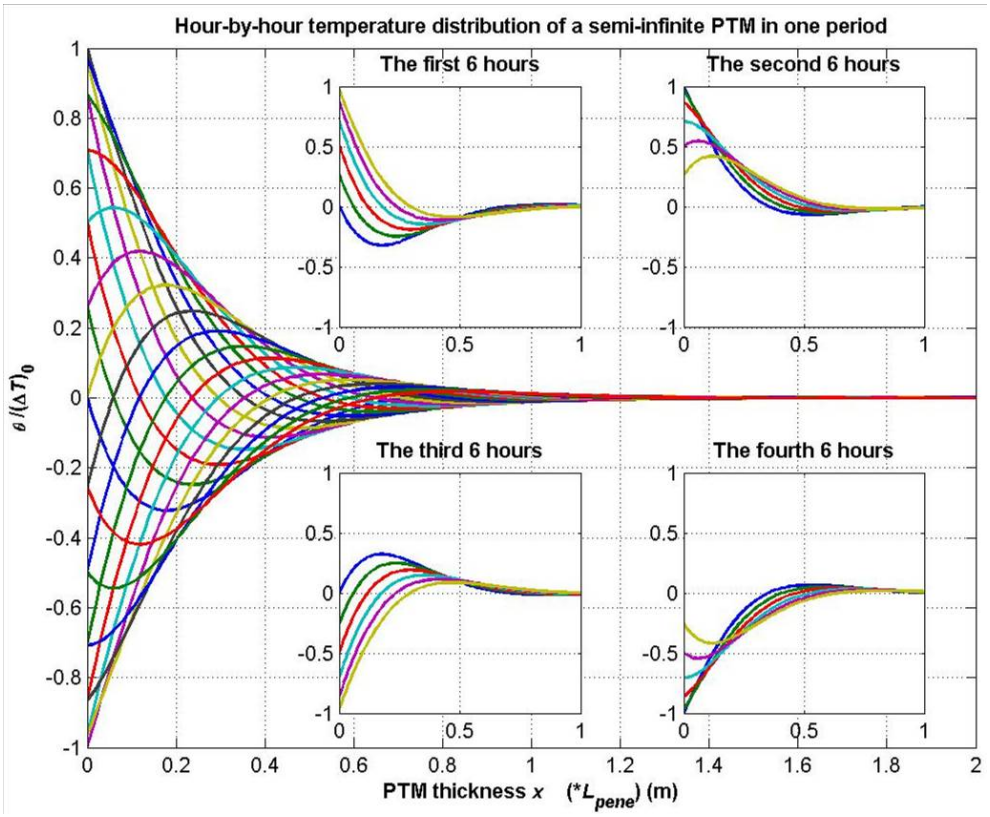

Figure 2.2—Hour-by-hour temperature distributions of a semi-infinite PTM in one period

From the Fourier's Law of heat conduction for a one-dimensional system

$$q'' = -k\frac{\partial T}{\partial x} = -k\frac{\partial \theta}{\partial x} \tag{2. 26}$$

the heat flux q'' [W/m^2] at any distance x from the surface can be obtained:

$$q'' = -k\left\{(\Delta T)_0 e^{-\frac{\sqrt{2}\pi x}{L_{pene}}}\left(-\frac{\sqrt{2}\pi}{L_{pene}}\right)\left[\cos\left(\frac{2\pi t}{P}-\frac{\sqrt{2}\pi x}{L_{pene}}\right)+\sin\left(\frac{2\pi t}{P}-\frac{\sqrt{2}\pi x}{L_{pene}}\right)\right]\right\}$$

$$\Rightarrow q'' = k(\Delta T)_0 e^{-\frac{\sqrt{2}\pi x}{L_{pene}}}\frac{2\pi}{L_{pene}}\sin\left(\frac{2\pi t}{P}-\frac{\sqrt{2}\pi x}{L_{pene}}+\frac{\pi}{4}\right)$$

$$\Rightarrow q'' = \frac{2\pi k(\Delta T)_0}{L_{pene}} e^{-\frac{\sqrt{2}\pi x}{L_{pene}}}\sin\left(\frac{2\pi t}{P}-\frac{\sqrt{2}\pi x}{L_{pene}}+\frac{\pi}{4}\right) \tag{2. 27}$$

Let $x = 0$, and the heat flux at the surface is given by

$$q_0'' = \frac{2\pi k(\Delta T)_0}{L_{pene}}\sin\left(\frac{2\pi t}{P}+\frac{\pi}{4}\right) \tag{2. 28}$$

The surface heat flux is shown in Figure 2.3. The phase lag between the temperature and the heat flux at the surface is $P/8$.

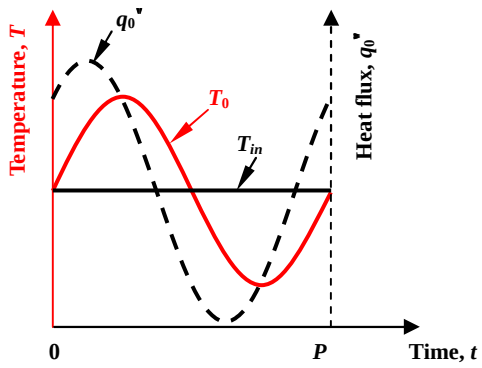

Figure 2.3—Surface temperature and heat flux variations

The amount of heat exchanged at the surface can be got as

$$\frac{Q_0}{A}=\int_{t_1}^{t_2} q_0'' dt=\frac{2\pi k\left(\Delta T\right)_0}{L_{pene}}\int_{t_1}^{t_2}\sin\left(\frac{2\pi t}{P}+\frac{\pi}{4}\right)dt=-\frac{2\pi\left(\Delta T\right)_0}{L_{pene}}\rho c_p\alpha\frac{P}{2\pi}\cos\left(\frac{2\pi t}{P}+\frac{\pi}{4}\right)\Bigg|_{t_1}^{t_2}$$

$$\Rightarrow\frac{Q_0}{A}=\frac{1}{2\pi}\rho c_p L_{pene}\left(\Delta T\right)_0\cos\left(\frac{2\pi t}{P}+\frac{\pi}{4}\right)\Bigg|_{t_2}^{t_1} \tag{2. 29}$$

where Q_0 [kJ] is the net heat exchanged between the semi-infinite PTM and the environment from t_1 to t_2.

Thus the amount of net-in or net-out heat per unit area of the PTM in one period is

$$\frac{Q_{0\,max}}{A}=\frac{1}{2\pi}\rho c_p L_{pene}\left(\Delta T\right)_0\left[1-\left(-1\right)\right]=\frac{1}{\pi}\rho c_p L_{pene}\left(\Delta T\right)_0 \tag{2. 30}$$

when $t_1=\frac{7P}{8}\pm nP$ and $t_2=\frac{3P}{8}\pm nP$, where $n=0,1,2,3,\ldots$.

It means that in one period, the total amount of heat transferred into or out of unit area of the PTM $Q_{0\,max}$ is $\rho c_p L_{pene}\left(\Delta T\right)_0/\pi$ (the net heat exchange between the PTM and the environment is zero in one period). Take one period for example, when

$t \in (-P/8, 3P/8)$, heat flows into the PTM (Since it is periodical, it can also be written as $t \in (0, 3P/8) \cup (7P/8, P)$; Here, the symbol "$\in$" is to be read "belongs to" or, more formally, as "is an element of the set" and the symbol "$\cup$" means "the union of" two sets.); and when $t \in (3P/8, 7P/8)$, heat flows out of the PTM.

From the definitions of mass specific heat c_p and volumetric specific heat c_{vol}, we know that $Q = mc_p\Delta T$ and $Q = Vc_{vol}\Delta T$, and thus we can define area heat capacity c_{area} as $Q = Ac_{area}\Delta T$. However, it is not very proper to be used in the field of architecture since buildings are usually under dynamic heating or cooling conditions. Therefore, in this thesis, we define **effective thickness** L^{eff} [m]:

$$L^{eff} \equiv \frac{L_{pene}}{\pi} = \sqrt{\frac{2\alpha P}{\pi}} \tag{2. 31}$$

and **effective area specific heat** c_{area}^{eff} [kJ/m^2·K]:

$$c_{area}^{eff} \equiv \rho c_p L^{eff} = \frac{\rho c_p L_{pene}}{\pi} \tag{2. 32}$$

and **effective heat exchange coefficient** ζ^0:

$$\zeta^0 \equiv \frac{Q_{0\,max}}{Ac_{area}^{eff}(\Delta T)_0} \tag{2. 33}$$

For the semi-infinite PTM described above, ζ^0 is equal to 1.

Some definitions of properties, parameters and coefficients are listed in Table 1.

Table 1—Definitions of properties, parameters and coefficients

Parameters	**Symbols or definitions**	**Units**	**Eqns.**
Conductivity	k	W/m·K	
Density	ρ	kg/m^3	
Mass	m	kg	
Heat transfer coefficient	h	W/m^2·K	
Mass specific heat	$c_p = \frac{Q}{m\Delta T}$	kJ/kg·K	(1. 1)
Thermal diffusivity	$\alpha = \frac{k}{\rho c_p}$	m^2/s	
Penetration depth	$L_{pene} \equiv \sqrt{2\pi\alpha P}$	m	(2. 23)
Volumetric specific heat	$c_{vol} = \frac{Q}{V\Delta T} = \rho c_p$	kJ/m^3·K	(1. 1)
Effective thickness	$L^{eff} \equiv \frac{L_{pene}}{\pi} = \sqrt{\frac{2\alpha P}{\pi}}$	m	(2. 31)
Area specific heat	$c_{area} = \frac{Q}{A\Delta T} = \rho c_p L$	kJ/m^2·K	
Effective area specific heat	$c_{area}^{eff} \equiv \rho c_p L^{eff} = \frac{\rho c_p L_{pene}}{\pi}$	kJ/m^2·K	(2. 32)
Effective heat exchange coefficient	$\zeta^0 \equiv \frac{Q_{0\,max}}{A c_{area}^{eff} \left(\Delta T\right)_0}$	dimensionless	(2. 33)

Thermo-physical properties of some common building materials are listed in Table 2.

Table 2—Thermo-physical properties of some common building materials

Materials	Conductivity	Density	Mass specific heat	Volumetric specific heat	Thermal diffusivity
	k	ρ	c_p	$c_{vol} = \rho c_p$	$\alpha = k/(\rho c_p)$
	[W/m·K]	[kg/m^3]	[kJ/kg·K]	[kJ/m^3·K]	[m^2/s]
Wood (Fir, pine or similar soft wood)	0.12	510	1.382	704.82	1.7026×10^{-7}
Normal-weight Concrete	1.90	2320	0.795	1844.40	1.0301×10^{-6}
Building Brick	0.73	1920	0.921	1768.32	4.1282×10^{-7}
Structural lightweight concrete	0.61	1600	0.921	1473.60	4.1395×10^{-7}
Insulating lightweight concrete	0.14	480	1.000	480.00	2.9167×10^{-7}
Face brick	1.30	2080	1.000	2080.00	6.2500×10^{-7}
Mineral fiber (loosefill)	0.048	9.6	0.712	6.84	7.0225×10^{-6}
Glass fiberboard (resin binder)	0.042	240	0.712	170.88	2.4579×10^{-7}
Expanded polystyrene	0.029	35	1.214	42.49	6.8251×10^{-7}
Gypsum board	0.16	800	1.089	871.20	1.8365×10^{-7}
Steel	45.30	7830	0.502	3930.66	1.1525×10^{-5}

Note: The values of the conductivity, the density and the specific heat are from reference [6]: page 4; however, values of the thermal diffusivity are calculated with the equation $\alpha = k/\left(\rho c_p\right)$ and are a little different from values given by reference [6] (where only two significant figures are left).

Values of some definitions of different building materials are shown in Table 3. Note: the period P of the thermal wave at the left surface of the PTMs is 24 hours.

Table 3—Values of some definitions of different building materials

Material	Penetration depth	Effective thickness	Effective area specific heat
	$L_{pene} \equiv \sqrt{2\pi\alpha P}$	$L^{eff} \equiv L_{pene} / \pi$	$c_{area}^{eff} \equiv \rho c_p L^{eff}$
	[m]	[m]	[kJ/m^2·K]
Wood (Fir, pine or similar soft wood)	0.3040	0.0968	68.207
Normal-weight Concrete	0.7478	0.2380	439.037
Building Brick	0.4734	0.1507	266.464
Structural lightweight concrete	0.4740	0.1509	222.357
Insulating lightweight concrete	0.3979	0.1267	60.797
Face brick	0.5825	0.1854	385.656
Mineral fiber (loosefill)	1.9525	0.6215	4.248
Glass fiberboard (resin binder)	0.3653	0.1163	19.869
Expanded polystyrene	0.6087	0.1938	8.233
Gypsum board	0.3158	0.1005	87.562
Steel	2.5013	0.7962	3129.528

Chapter 3: Dynamic Heat Transfer of Finite-thickness PTMs When $T_{inside\ air} = T_m$

3.1 Problem description

Actual building PTMs are not semi-*infinite*. Therefore, in this chapter, we will discuss the dynamic heat transfer problem of finite-thickness PTMs. In these cases, it is necessary to consider the B.C. at the right surfaces of the PTMs. Without considering heat transfer by radiation, three kinds of B.C.s exist here: **prescribed boundary temperature**, **prescribed heat flux** and **heat transfer by convection**, which are also called the **boundary condition of the first**, **second** and **third kind**, respectively. In this thesis, we will consider the B.C.s expressed as follows

First kind: $$T(L,t) = T_L \tag{3. 1}$$

Second kind: $$-k\left(\frac{\partial T}{\partial x}\right)_L = q_L^{"} \tag{3. 2}$$

Third kind: $$-k\left(\frac{\partial T}{\partial x}\right)_L = h\left[T(L,t) - T_{inside\ air}\right] \tag{3. 3}$$

where h [W/m^2·K] is called **heat transfer coefficient**, **film conductance**, or **film coefficient**. Since the **thermal resistance** (R-Value) of the indoor air film is typically R-0.7[5] (0.1234 m^2·K/W), it is easy to get $h = 1/R = 8.1037$ W/m^2·K. Generally, the inside air temperature $T_{inside\ air}$ is not equal to T_m and $T_{inside\ air}$ is not constant. However, if the amount of the inside air is large enough, $T_{inside\ air}$ can be considered as constant,

except inside air near the building envelope (where air temperature floats under the influence of the outside surface thermal wave); alternatively, suppose that there is a "virtual heat sink/source" in the building, which can immediately and exactly absorb/release the same amount of heat transferred into/out of the inside air, and then $T_{inside\ air}$ will be constant. In this thesis, we treat $T_{inside\ air}$ as constant. Under this assumption, first in this chapter, let $T_{inside\ air}$ equal to T_m and deduce the exact solution of the problem; then in Chapter 4, let $T_{inside\ air}$ not equal to T_m and get some results by numerical method.

For actual building PTMs, the B.C. of the third kind is much more common and also more important. And note: if $h \to \infty$, since the temperature gradient at the right surface must be finite, we can get $\left[T\left(L,t\right)-T_{inside\ air}\right]\to 0$ or $T\left(L,t\right)\to T_{inside\ air}$, and the B.C. of the third kind reduces to that of the first kind; if $h \to 0$, the B.C. of the third kind reduces to the simplest case of the B.C. of the second kind, that is, $q_L^{"}=0$, since $T\left(L,t\right)-T_{inside\ air}$ is finite. Therefore, in this thesis, we will first solve the problem with the B.C. of the third kind using the same method described in Chapter 2, and then reduce it to the other two kinds.

3.2 Mathematical deduction

3.2.1 Basic deduction

When $T_{inside\ air}=T_m$, since $\theta\left(x,t\right)=T\left(x,t\right)-T_m$, the B.C. of the third kind can be

rewritten as

$$\left(\frac{\partial\theta}{\partial x}\right)_L = -\frac{h}{k}\theta(L,t) \tag{3. 4}$$

Using the method described in the previous chapter, it is easy to know that

1) The differential equation is the same as Eqn. (2. 12) and its general solution is

$$\theta_c(x,t) = \left(C_1 e^{\sqrt{\frac{2i\pi}{\alpha P}}x} + C_2 e^{-\sqrt{\frac{2i\pi}{\alpha P}}x}\right) e^{\frac{2i\pi}{P}t} \tag{3. 5}$$

2) The B.C. at the left surfaces is still Eqn. (2. 14), which yields

$$C_1 + C_2 = (\Delta T)_0 \tag{3. 6}$$

3) The only change of the problem is Eqn. (2. 13), which becomes

$$\left(\frac{\partial\theta_c}{\partial x}\right)_L = -\frac{h}{k}\theta_c(L,t) \tag{3. 7}$$

$$\Rightarrow \left(C_1\sqrt{\frac{2i\pi}{\alpha P}}e^{\sqrt{\frac{2i\pi}{\alpha P}}x} - C_2\sqrt{\frac{2i\pi}{\alpha P}}e^{-\sqrt{\frac{2i\pi}{\alpha P}}x}\right)e^{\frac{2i\pi}{P}t}\Bigg|_L = -\frac{h}{k}\left(C_1 e^{\sqrt{\frac{2i\pi}{\alpha P}}x} + C_2 e^{-\sqrt{\frac{2i\pi}{\alpha P}}x}\right)e^{\frac{2i\pi}{P}t}\Bigg|_L$$

$$\Rightarrow \sqrt{\frac{2i\pi}{\alpha P}}\left(C_1 e^{\sqrt{\frac{2i\pi}{\alpha P}}L} - C_2 e^{-\sqrt{\frac{2i\pi}{\alpha P}}L}\right) = -\frac{h}{k}\left(C_1 e^{\sqrt{\frac{2i\pi}{\alpha P}}L} + C_2 e^{-\sqrt{\frac{2i\pi}{\alpha P}}L}\right)$$

$$\Rightarrow (1+i)\sqrt{\frac{\pi}{\alpha P}}\left(C_1 e^{(1+i)\sqrt{\frac{\pi}{\alpha P}}L} - C_2 e^{-(1+i)\sqrt{\frac{\pi}{\alpha P}}L}\right) = -\frac{h}{k}\left(C_1 e^{(1+i)\sqrt{\frac{\pi}{\alpha P}}L} + C_2 e^{-(1+i)\sqrt{\frac{\pi}{\alpha P}}L}\right)$$

From previous definitions, we can get $\sqrt{\frac{\pi}{\alpha P}} = \frac{\sqrt{2}\pi}{L_{pene}} = \frac{\sqrt{2}}{L^{eff}}$; Let

$$\delta \equiv \frac{\sqrt{2}L}{L^{eff}} \tag{3. 8}$$

which can be called **Dimensionless Thickness**, and then we can get

$$(1+i)\frac{\sqrt{2}}{L^{eff}}\left(C_1 e^{(1+i)\delta} - C_2 e^{-(1+i)\delta}\right) = -\frac{h}{k}\left(C_1 e^{(1+i)\delta} + C_2 e^{-(1+i)\delta}\right)$$

$$\Rightarrow \frac{\sqrt{2}(1+i)}{L^{eff}}\left\{C_1 e^{(1+i)\delta} - \left[(\Delta T)_0 - C_1\right] e^{-(1+i)\delta}\right\} = -\frac{h}{k}\left\{C_1 e^{(1+i)\delta} + \left[(\Delta T)_0 - C_1\right] e^{-(1+i)\delta}\right\}$$

$$\Rightarrow \left\{\left[\frac{\sqrt{2}(1+i)}{L^{eff}} + \frac{h}{k}\right] e^{(1+i)\delta} + \left[\frac{\sqrt{2}(1+i)}{L^{eff}} - \frac{h}{k}\right] e^{-(1+i)\delta}\right\} C_1 = (\Delta T)_0 \left[\frac{\sqrt{2}(1+i)}{L^{eff}} - \frac{h}{k}\right] e^{-(1+i)\delta}$$

$$\Rightarrow C_1 = \frac{(\Delta T)_0}{\frac{\sqrt{2}(1+i)k + hL^{eff}}{\sqrt{2}(1+i)k - hL^{eff}} e^{2(1+i)\delta} + 1} = \frac{(\Delta T)_0}{\frac{(1+i)+\varepsilon}{(1+i)-\varepsilon} e^{2(1+i)\delta} + 1}$$

$$\Rightarrow C_1 = \frac{(1-\varepsilon+i)}{(1+\varepsilon+i)e^{2(1+i)\delta} + (1-\varepsilon+i)}(\Delta T)_0 \tag{3. 9}$$

$$\Rightarrow C_2 = (\Delta T)_0 - C_1 = \frac{(1+\varepsilon+i)e^{2(1+i)\delta}}{(1+\varepsilon+i)e^{2(1+i)\delta} + (1-\varepsilon+i)}(\Delta T)_0 \tag{3. 10}$$

where $\varepsilon \equiv \frac{hL^{eff}}{\sqrt{2}k} = \frac{hL_{pene}}{\sqrt{2}\pi k}$ (3. 11)

which is a dimensionless parameter called **Dynamic Biot Number** in this thesis. Then

$$\theta_c(x,t) = (\Delta T)_0 \left\{ \begin{array}{l} \frac{(1-\varepsilon+i)}{(1+\varepsilon+i)e^{2(1+i)\delta} + (1-\varepsilon+i)} e^{(1+i)\sqrt{\frac{\pi}{\alpha P}}x} \\ + \frac{(1+\varepsilon+i)e^{2(1+i)\delta}}{(1+\varepsilon+i)e^{2(1+i)\delta} + (1-\varepsilon+i)} e^{-(1+i)\sqrt{\frac{\pi}{\alpha P}}x} \end{array} \right\} e^{\frac{2i\pi t}{P}}$$

$$\Rightarrow \theta_c(x,t) = (\Delta T)_0 \frac{(1-\varepsilon+i)e^{(1+i)\frac{\sqrt{2}x}{L^{eff}}} e^{\frac{2i\pi t}{P}} + (1+\varepsilon+i)e^{2(1+i)\delta} e^{-(1+i)\frac{\sqrt{2}x}{L^{eff}}} e^{\frac{2i\pi t}{P}}}{(1+\varepsilon+i)e^{2(1+i)\delta} + (1-\varepsilon+i)}$$

$$\Rightarrow \theta_c(x,t) = (\Delta T)_0 \frac{(1-\varepsilon+i)e^{\frac{\sqrt{2}x}{L^{eff}}} e^{i\left(\frac{\sqrt{2}x}{L^{eff}} + \frac{2\pi t}{P}\right)} + (1+\varepsilon+i)e^{\left(2\delta - \frac{\sqrt{2}x}{L^{eff}}\right)} e^{i\left(2\delta - \frac{\sqrt{2}x}{L^{eff}} + \frac{2\pi t}{P}\right)}}{(1+\varepsilon+i)e^{2\delta}e^{2i\delta} + (1-\varepsilon+i)}$$

$$\Rightarrow \theta_c(x,t) = (\Delta T)_0 \frac{\left\{ \begin{array}{l} (1-\varepsilon+i)e^{\frac{\sqrt{2}x}{L^{eff}}}\left[\cos\left(\frac{\sqrt{2}x}{L^{eff}}+\frac{2\pi t}{P}\right)+i\sin\left(\frac{\sqrt{2}x}{L^{eff}}+\frac{2\pi t}{P}\right)\right] \\ +(1+\varepsilon+i)e^{\left(2\delta-\frac{\sqrt{2}x}{L^{eff}}\right)}\left[\cos\left(2\delta-\frac{\sqrt{2}x}{L^{eff}}+\frac{2\pi t}{P}\right)+i\sin\left(2\delta-\frac{\sqrt{2}x}{L^{eff}}+\frac{2\pi t}{P}\right)\right] \end{array} \right\}}{(1+\varepsilon+i)e^{2\delta}\left[\cos(2\delta)+i\sin(2\delta)\right]+(1-\varepsilon+i)}$$

$$\Rightarrow \theta_c(x,t) = (\Delta T)_0 \frac{\left\{ \begin{array}{l} e^{\frac{\sqrt{2}x}{L^{eff}}}\left[(1-\varepsilon)\cos\left(\frac{\sqrt{2}x}{L^{eff}}+\frac{2\pi t}{P}\right)-\sin\left(\frac{\sqrt{2}x}{L^{eff}}+\frac{2\pi t}{P}\right)\right] \\ +ie^{\frac{\sqrt{2}x}{L^{eff}}}\left[\cos\left(\frac{\sqrt{2}x}{L^{eff}}+\frac{2\pi t}{P}\right)+(1-\varepsilon)\sin\left(\frac{\sqrt{2}x}{L^{eff}}+\frac{2\pi t}{P}\right)\right] \\ +e^{\left(2\delta-\frac{\sqrt{2}x}{L^{eff}}\right)}\left[(1+\varepsilon)\cos\left(2\delta-\frac{\sqrt{2}x}{L^{eff}}+\frac{2\pi t}{P}\right)-\sin\left(2\delta-\frac{\sqrt{2}x}{L^{eff}}+\frac{2\pi t}{P}\right)\right] \\ +ie^{\left(2\delta-\frac{\sqrt{2}x}{L^{eff}}\right)}\left[\cos\left(2\delta-\frac{\sqrt{2}x}{L^{eff}}+\frac{2\pi t}{P}\right)+(1+\varepsilon)\sin\left(2\delta-\frac{\sqrt{2}x}{L^{eff}}+\frac{2\pi t}{P}\right)\right] \end{array} \right\}}{e^{2\delta}\left[(1+\varepsilon)\cos(2\delta)-\sin(2\delta)\right]+ie^{2\delta}\left[\cos(2\delta)+(1+\varepsilon)\sin(2\delta)\right]+(1-\varepsilon)+i}$$

$$\Rightarrow \theta_c(x,t) = (\Delta T)_0 \frac{A_1+iA_2}{B_1+iB_2} = (\Delta T)_0 \frac{(A_1B_1+A_2B_2)+i(A_2B_1-A_1B_2)}{B_1^2+B_2^2} \qquad (3.12)$$

where $A_1 = \left\{ \begin{array}{l} e^{\frac{\sqrt{2}x}{L^{eff}}}\left[(1-\varepsilon)\cos\left(\frac{\sqrt{2}x}{L^{eff}}+\frac{2\pi t}{P}\right)-\sin\left(\frac{\sqrt{2}x}{L^{eff}}+\frac{2\pi t}{P}\right)\right] \\ +e^{\left(2\delta-\frac{\sqrt{2}x}{L^{eff}}\right)}\left[(1+\varepsilon)\cos\left(2\delta-\frac{\sqrt{2}x}{L^{eff}}+\frac{2\pi t}{P}\right)-\sin\left(2\delta-\frac{\sqrt{2}x}{L^{eff}}+\frac{2\pi t}{P}\right)\right] \end{array} \right\}$

$$\Rightarrow A_1 = \left\{ \begin{array}{l} \varepsilon\left[e^{\left(2\delta-\frac{\sqrt{2}x}{L^{eff}}\right)}\cos\left(2\delta-\frac{\sqrt{2}x}{L^{eff}}+\frac{2\pi t}{P}\right)-e^{\frac{\sqrt{2}x}{L^{eff}}}\cos\left(\frac{\sqrt{2}x}{L^{eff}}+\frac{2\pi t}{P}\right)\right] \\ +\sqrt{2}\left[e^{\left(2\delta-\frac{\sqrt{2}x}{L^{eff}}\right)}\cos\left(2\delta-\frac{\sqrt{2}x}{L^{eff}}+\frac{2\pi t}{P}+\frac{\pi}{4}\right)+e^{\frac{\sqrt{2}x}{L^{eff}}}\cos\left(\frac{\sqrt{2}x}{L^{eff}}+\frac{2\pi t}{P}+\frac{\pi}{4}\right)\right] \end{array} \right\} \qquad (3.13)$$

and $A_2 = \left\{ \begin{array}{l} e^{\frac{\sqrt{2}x}{L^{eff}}}\left[\cos\left(\frac{\sqrt{2}x}{L^{eff}}+\frac{2\pi t}{P}\right)+(1-\varepsilon)\sin\left(\frac{\sqrt{2}x}{L^{eff}}+\frac{2\pi t}{P}\right)\right] \\ +e^{\left(2\delta-\frac{\sqrt{2}x}{L^{eff}}\right)}\left[\cos\left(2\delta-\frac{\sqrt{2}x}{L^{eff}}+\frac{2\pi t}{P}\right)+(1+\varepsilon)\sin\left(2\delta-\frac{\sqrt{2}x}{L^{eff}}+\frac{2\pi t}{P}\right)\right] \end{array} \right\}$

$$\Rightarrow A_2=\left\{\begin{array}{l}\varepsilon\left[e^{\left(2\delta-\frac{\sqrt{2}x}{L^{eff}}\right)}\sin\left(2\delta-\frac{\sqrt{2}x}{L^{eff}}+\frac{2\pi t}{P}\right)-e^{\frac{\sqrt{2}x}{L^{eff}}}\sin\left(\frac{\sqrt{2}x}{L^{eff}}+\frac{2\pi t}{P}\right)\right]\\ +\sqrt{2}\left[e^{\left(2\delta-\frac{\sqrt{2}x}{L^{eff}}\right)}\sin\left(2\delta-\frac{\sqrt{2}x}{L^{eff}}+\frac{2\pi t}{P}+\frac{\pi}{4}\right)+e^{\frac{\sqrt{2}x}{L^{eff}}}\sin\left(\frac{\sqrt{2}x}{L^{eff}}+\frac{2\pi t}{P}+\frac{\pi}{4}\right)\right]\end{array}\right\} \quad (3.\ 14)$$

and $B_1=(1+\varepsilon)e^{2\delta}\cos(2\delta)-e^{2\delta}\sin(2\delta)+(1-\varepsilon)$

$$\Rightarrow B_1=\varepsilon\left[e^{2\delta}\cos(2\delta)-1\right]+\left[e^{2\delta}\cos(2\delta)-e^{2\delta}\sin(2\delta)+1\right] \quad (3.\ 15)$$

and $B_2=e^{2\delta}\cos(2\delta)+(1+\varepsilon)e^{2\delta}\sin(2\delta)+1$

$$\Rightarrow B_2=\varepsilon\left[e^{2\delta}\sin(2\delta)\right]+\left[e^{2\delta}\cos(2\delta)+e^{2\delta}\sin(2\delta)+1\right] \quad (3.\ 16)$$

Then we can get

$$\theta(x,t)=(\Delta T)_0\frac{A_2B_1-A_1B_2}{B_1^2+B_2^2} \quad (3.\ 17)$$

3.2.2 Heat exchange between the PTMs and the outside environment

Since A_1 and A_2 are functions of x and B_1 and B_2 are not,

$$q^{"}=-k\frac{\partial T}{\partial x}=-k\frac{\partial\theta}{\partial x}=-k\frac{(\Delta T)_0}{B_1^2+B_2^2}\left(B_1\frac{\partial A_2}{\partial x}-B_2\frac{\partial A_1}{\partial x}\right) \quad (3.\ 18)$$

where

$$\frac{\partial A_1}{\partial x}=\frac{2}{L^{eff}}\left\{\begin{array}{l}\varepsilon\left[e^{\left(2\delta-\frac{\sqrt{2}x}{L^{eff}}\right)}\sin\left(2\delta-\frac{\sqrt{2}x}{L^{eff}}+\frac{2\pi t}{P}-\frac{\pi}{4}\right)+e^{\frac{\sqrt{2}x}{L^{eff}}}\sin\left(\frac{\sqrt{2}x}{L^{eff}}+\frac{2\pi t}{P}-\frac{\pi}{4}\right)\right]\\ +\sqrt{2}\left[e^{\left(2\delta-\frac{\sqrt{2}x}{L^{eff}}\right)}\sin\left(2\delta-\frac{\sqrt{2}x}{L^{eff}}+\frac{2\pi t}{P}\right)-e^{\frac{\sqrt{2}x}{L^{eff}}}\sin\left(\frac{\sqrt{2}x}{L^{eff}}+\frac{2\pi t}{P}\right)\right]\end{array}\right\} \quad (3.\ 19)$$

and

$$\frac{\partial A_2}{\partial x}=\frac{-2}{L^{eff}}\left\{\begin{array}{l}\varepsilon\left[e^{\left(2\delta-\frac{\sqrt{2}x}{L^{eff}}\right)}\cos\left(2\delta-\frac{\sqrt{2}x}{L^{eff}}+\frac{2\pi t}{P}-\frac{\pi}{4}\right)+e^{\frac{\sqrt{2}x}{L^{eff}}}\cos\left(\frac{\sqrt{2}x}{L^{eff}}+\frac{2\pi t}{P}-\frac{\pi}{4}\right)\right]\\ +\sqrt{2}\left[e^{\left(2\delta-\frac{\sqrt{2}x}{L^{eff}}\right)}\cos\left(2\delta-\frac{\sqrt{2}x}{L^{eff}}+\frac{2\pi t}{P}\right)-e^{\frac{\sqrt{2}x}{L^{eff}}}\cos\left(\frac{\sqrt{2}x}{L^{eff}}+\frac{2\pi t}{P}\right)\right]\end{array}\right\} \quad (3.\ 20)$$

Let $x=0$, and the heat flux at the left surfaces is given by

$$q_0^{"}=-k\frac{(\Delta T)_0}{B_1^{\ 2}+B_2^{\ 2}}\left[B_1\left(\frac{\partial A_2}{\partial x}\right)_0-\left(B_2\frac{\partial A_1}{\partial x}\right)_0\right] \quad (3.\ 21)$$

where $\left(\frac{\partial A_1}{\partial x}\right)_0=\frac{2}{L^{eff}}\left\{\begin{array}{l}\varepsilon\left[e^{2\delta}\sin\left(2\delta+\frac{2\pi t}{P}-\frac{\pi}{4}\right)+\sin\left(\frac{2\pi t}{P}-\frac{\pi}{4}\right)\right]\\ +\sqrt{2}\left[e^{2\delta}\sin\left(2\delta+\frac{2\pi t}{P}\right)-\sin\left(\frac{2\pi t}{P}\right)\right]\end{array}\right\}$

$$\Rightarrow\left(\frac{\partial A_1}{\partial x}\right)_0=\frac{\sqrt{2}}{L^{eff}}\left\{\begin{array}{l}\left[\varepsilon\left(e^{2\delta}\sin 2\delta+e^{2\delta}\cos 2\delta+1\right)+2\left(e^{2\delta}\cos 2\delta-1\right)\right]\sin\left(\frac{2\pi t}{P}\right)\\ +\left[\varepsilon\left(e^{2\delta}\sin 2\delta-e^{2\delta}\cos 2\delta-1\right)+2e^{2\delta}\sin\left(2\delta\right)\right]\cos\left(\frac{2\pi t}{P}\right)\end{array}\right\}$$

$$\Rightarrow\left(\frac{\partial A_1}{\partial x}\right)_0=\frac{\sqrt{2}}{L^{eff}}\left[D_1\sin\left(\frac{2\pi t}{P}\right)+D_2\cos\left(\frac{2\pi t}{P}\right)\right] \quad (3.\ 22)$$

and $\left(\frac{\partial A_2}{\partial x}\right)_0=\frac{-2}{L^{eff}}\left\{\begin{array}{l}\varepsilon\left[e^{2\delta}\cos\left(2\delta+\frac{2\pi t}{P}-\frac{\pi}{4}\right)+\cos\left(\frac{2\pi t}{P}-\frac{\pi}{4}\right)\right]\\ +\sqrt{2}\left[e^{2\delta}\cos\left(2\delta+\frac{2\pi t}{P}\right)-\cos\left(\frac{2\pi t}{P}\right)\right]\end{array}\right\}$

$$\Rightarrow\left(\frac{\partial A_2}{\partial x}\right)_0=\frac{\sqrt{2}}{L^{eff}}\left\{\begin{array}{l}\left[\varepsilon\left(e^{2\delta}\sin 2\delta-e^{2\delta}\cos 2\delta-1\right)+2e^{2\delta}\sin 2\delta\right]\sin\left(\frac{2\pi t}{P}\right)\\ -\left[\varepsilon\left(e^{2\delta}\sin 2\delta+e^{2\delta}\cos 2\delta+1\right)+2\left(e^{2\delta}\cos 2\delta-1\right)\right]\cos\left(\frac{2\pi t}{P}\right)\end{array}\right\}$$

$$\Rightarrow\left(\frac{\partial A_2}{\partial x}\right)_0=\frac{\sqrt{2}}{L^{eff}}\left[D_2\sin\left(\frac{2\pi t}{P}\right)-D_1\cos\left(\frac{2\pi t}{P}\right)\right] \quad (3.\ 23)$$

where $D_1=\varepsilon\left(e^{2\delta}\sin 2\delta+e^{2\delta}\cos 2\delta+1\right)+2\left(e^{2\delta}\cos 2\delta-1\right)$ (3. 24)

and $D_2 = \varepsilon\left(e^{2\delta}\sin 2\delta - e^{2\delta}\cos 2\delta - 1\right) + 2e^{2\delta}\sin\left(2\delta\right)$ (3. 25)

Therefore,

$$q_0^{"} = -k\frac{\left(\Delta T\right)_0}{B_1^2 + B_2^2}\frac{\sqrt{2}}{L^{eff}}\left\{B_1\left[D_2\sin\left(\frac{2\pi t}{P}\right) - D_1\cos\left(\frac{2\pi t}{P}\right)\right] - B_2\left[D_1\sin\left(\frac{2\pi t}{P}\right) + D_2\cos\left(\frac{2\pi t}{P}\right)\right]\right\}$$

$$\Rightarrow q_0^{"} = -k\frac{\sqrt{2}}{L^{eff}}\frac{\left(\Delta T\right)_0}{B_1^2 + B_2^2}\left\{\left(B_1D_2 - B_2D_1\right)\sin\left(\frac{2\pi t}{P}\right) - \left(B_1D_1 + B_2D_2\right)\cos\left(\frac{2\pi t}{P}\right)\right\}$$

$$\Rightarrow q_0^{"} = -\frac{\sqrt{2}k\left(\Delta T\right)_0}{L^{eff}}\frac{\sqrt{\left(B_1D_2 - B_2D_1\right)^2 + \left(B_1D_1 + B_2D_2\right)^2}}{B_1^2 + B_2^2}\sin\left(\frac{2\pi t}{P} - \varphi_0\right)$$

$$\Rightarrow q_0^{"} = -\frac{\sqrt{2}k\left(\Delta T\right)_0}{L^{eff}}\sqrt{\frac{D_1^2 + D_2^2}{B_1^2 + B_2^2}}\sin\left(\frac{2\pi t}{P} - \varphi_0\right) \quad (3.\ 26)$$

where $\tan\varphi_0 = \dfrac{B_1D_1 + B_2D_2}{B_1D_2 - B_2D_1}$ (3. 27)

When $q_0^{"} = 0$,

$$t_0 = \frac{P}{2\pi}\varphi_0 = \frac{P}{2\pi}\left[\tan^{-1}\left(\frac{B_1D_1 + B_2D_2}{B_1D_2 - B_2D_1}\right) \pm n\pi\right] = \frac{P}{2\pi}\tan^{-1}\left(\frac{B_1D_1 + B_2D_2}{B_1D_2 - B_2D_1}\right) \pm \frac{nP}{2} \quad (3.\ 28)$$

where $n = 0, 1, 2, 3, \ldots$.

Note: In every period, there are two times ($t = t_{01}$ and $t = t_{02} = t_{01} + P/2$) that $q_0^{"} = 0$. Suppose that heat begins to flow into the PTMs from the outside environment at t_{01}, and half period later, at t_{02}, the direction of the heat flow will reverse and heat will begin to flow out of the PTMs. See Figure 2.3, for the case of the semi-infinite PTM.

The amount of heat exchanged from t_1 to t_2 at the left surfaces can be got as

$$\frac{Q_0}{A} = \int_{t_1}^{t_2} q_0^{"}dt = -\frac{\sqrt{2}k\left(\Delta T\right)_0}{L^{eff}}\sqrt{\frac{D_1^2 + D_2^2}{B_1^2 + B_2^2}}\int_{t_1}^{t_2}\sin\left(\frac{2\pi t}{P} - \varphi_0\right)dt$$

$$\Rightarrow \frac{Q_0}{A} = \frac{\sqrt{2}k\left(\Delta T\right)_0}{L^{eff}} \sqrt{\frac{D_1^2 + D_2^2}{B_1^2 + B_2^2}} \frac{P}{2\pi} \cos\left(\frac{2\pi t}{P} - \varphi_0\right)\Bigg|_{t_1}^{t_2}$$

$$\Rightarrow \frac{Q_0}{A} = \frac{\sqrt{2}}{4} \sqrt{\frac{D_1^2 + D_2^2}{B_1^2 + B_2^2}} \rho c_p L^{eff} \left(\Delta T\right)_0 \cos\left(\frac{2\pi t}{P} - \varphi_0\right)\Bigg|_{t_1}^{t_2}$$

$$\Rightarrow \frac{Q_0}{A} = \frac{1}{2}\zeta_{\varepsilon,\delta}^0 c_{area}^{eff} \left(\Delta T\right)_0 \cos\left(\frac{2\pi t}{P} - \varphi_0\right)\Bigg|_{t_1}^{t_2} \tag{3. 29}$$

where $\zeta_{\varepsilon,\delta}^0 = \frac{\sqrt{2}}{2} \sqrt{\frac{D_1^2 + D_2^2}{B_1^2 + B_2^2}}$ (3. 30)

which is the **Effective Heat Exchange Coefficient** for certain ε and δ.

3.2.3 Heat storage of the PTMs

In heating processes, all the heat transferred at the left surfaces are stored in the PTMs for cases of $\varepsilon = 0$ (thermally insulated), since there is no heat exchanged at the right surfaces. However, for other cases, heat is not all stored in the PTMs since it is also transferred into building interior spaces at the right surfaces of the PTMs. Detailed deduction is as follows.

Let $x = L$ in Eqn. (3. 18), and the heat flux at the right surfaces is given by

$$q_L^{"} = -k \frac{\left(\Delta T\right)_0}{B_1^{\,2} + B_2^{\,2}} \left[B_1 \left(\frac{\partial A_2}{\partial x}\right)_L - B_2 \left(\frac{\partial A_1}{\partial x}\right)_L \right] \tag{3. 31}$$

where $\left(\frac{\partial A_1}{\partial x}\right)_L = \frac{2}{L^{eff}} \left\{ \begin{array}{l} \varepsilon \left[e^{\delta} \sin\left(\delta + \frac{2\pi t}{P} - \frac{\pi}{4}\right) + e^{\delta} \sin\left(\delta + \frac{2\pi t}{P} - \frac{\pi}{4}\right) \right] \\ + \sqrt{2} \left[e^{\delta} \sin\left(\delta + \frac{2\pi t}{P}\right) - e^{\delta} \sin\left(\delta + \frac{2\pi t}{P}\right) \right] \end{array} \right\}$

$$\Rightarrow \left(\frac{\partial A_1}{\partial x}\right)_L = \frac{4\varepsilon}{L^{eff}} e^{\delta} \sin\left(\delta + \frac{2\pi t}{P} - \frac{\pi}{4}\right)$$

$$\Rightarrow \left(\frac{\partial A_1}{\partial x}\right)_L = \frac{\sqrt{2}}{L^{eff}} \left\{ 2\varepsilon e^{\delta} \left(\sin\delta + \cos\delta\right) \sin\left(\frac{2\pi t}{P}\right) + 2\varepsilon e^{\delta} \left(\sin\delta - \cos\delta\right) \cos\left(\frac{2\pi t}{P}\right) \right\}$$

$$\Rightarrow \left(\frac{\partial A_1}{\partial x}\right)_L = \frac{\sqrt{2}}{L^{eff}} \left[F_1 \sin\left(\frac{2\pi t}{P}\right) + F_2 \cos\left(\frac{2\pi t}{P}\right) \right] \qquad (3.\ 32)$$

and $$\left(\frac{\partial A_2}{\partial x}\right)_L = \frac{-2}{L^{eff}} \left\{ \begin{array}{l} \varepsilon \left[e^{\delta} \cos\left(\delta + \frac{2\pi t}{P} - \frac{\pi}{4}\right) + e^{\delta} \cos\left(\delta + \frac{2\pi t}{P} - \frac{\pi}{4}\right) \right] \\ + \sqrt{2} \left[e^{\delta} \cos\left(\delta + \frac{2\pi t}{P}\right) - e^{\delta} \cos\left(\delta + \frac{2\pi t}{P}\right) \right] \end{array} \right\}$$

$$\Rightarrow \left(\frac{\partial A_2}{\partial x}\right)_L = \frac{-4\varepsilon}{L^{eff}} e^{\delta} \cos\left(\delta + \frac{2\pi t}{P} - \frac{\pi}{4}\right)$$

$$\Rightarrow \left(\frac{\partial A_2}{\partial x}\right)_L = \frac{\sqrt{2}\varepsilon}{L^{eff}} \left\{ 2e^{\delta} \left(\sin\delta - \cos\delta\right) \sin\left(\frac{2\pi t}{P}\right) - 2e^{\delta} \left(\sin\delta + \cos\delta\right) \cos\left(\frac{2\pi t}{P}\right) \right\}$$

$$\Rightarrow \left(\frac{\partial A_2}{\partial x}\right)_L = \frac{\sqrt{2}}{L^{eff}} \left[F_2 \sin\left(\frac{2\pi t}{P}\right) - F_1 \cos\left(\frac{2\pi t}{P}\right) \right] \qquad (3.\ 33)$$

where $F_1 = 2\varepsilon e^{\delta} \left(\sin\delta + \cos\delta\right)$ (3. 34)

and $F_2 = 2\varepsilon e^{\delta} \left(\sin\delta - \cos\delta\right)$ (3. 35)

Therefore,

$$q_L^{"} = -k \frac{\left(\Delta T\right)_0}{B_1^{\,2} + B_2^{\,2}} \frac{\sqrt{2}}{L^{eff}} \left\{ B_1 \left[F_2 \sin\left(\frac{2\pi t}{P}\right) - F_1 \cos\left(\frac{2\pi t}{P}\right) \right] - B_2 \left[F_1 \sin\left(\frac{2\pi t}{P}\right) + F_2 \cos\left(\frac{2\pi t}{P}\right) \right] \right\}$$

$$\Rightarrow q_L^{"} = -k \frac{\left(\Delta T\right)_0}{B_1^{\,2} + B_2^{\,2}} \frac{\sqrt{2}}{L^{eff}} \left\{ \left(B_1 F_2 - B_2 F_1\right) \sin\left(\frac{2\pi t}{P}\right) - \left(B_1 F_1 + B_2 F_2\right) \cos\left(\frac{2\pi t}{P}\right) \right\}$$

$$\Rightarrow q_L^{"} = -\frac{\sqrt{2}k\left(\Delta T\right)_0}{L^{eff}}\frac{\sqrt{\left(B_1F_2 - B_2F_1\right)^2 + \left(B_1F_1 + B_2F_2\right)^2}}{B_1^2 + B_2^2}\sin\left(\frac{2\pi t}{P} - \varphi_L\right)$$

$$\Rightarrow q_L^{"} = -\frac{\sqrt{2}k\left(\Delta T\right)_0}{L^{eff}}\sqrt{\frac{F_1^2 + F_2^2}{B_1^2 + B_2^2}}\sin\left(\frac{2\pi t}{P} - \varphi_L\right) \tag{3. 36}$$

where $\tan\varphi_L = \dfrac{B_1F_1 + B_2F_2}{B_1F_2 - B_2F_1}$ (3. 37)

When $q_L^{"} = 0$,

$$t_L = \frac{P}{2\pi}\varphi_L = \frac{P}{2\pi}\left[\tan^{-1}\left(\frac{B_1F_1 + B_2F_2}{B_1F_2 - B_2F_1}\right) \pm n\pi\right] = \frac{P}{2\pi}\tan^{-1}\left(\frac{B_1F_1 + B_2F_2}{B_1F_2 - B_2F_1}\right) \pm \frac{nP}{2} \tag{3. 38}$$

The amount of heat exchanged from t_1 to t_2 at the right surfaces can be got as

$$\frac{Q_L}{A} = \int_{t_1}^{t_2} q_L^{"}dt = -\frac{\sqrt{2}k\left(\Delta T\right)_0}{L^{eff}}\sqrt{\frac{F_1^2 + F_2^2}{B_1^2 + B_2^2}}\int_{t_1}^{t_2}\sin\left(\frac{2\pi t}{P} - \varphi_L\right)dt$$

$$\Rightarrow \frac{Q_L}{A} = \frac{\sqrt{2}k\left(\Delta T\right)_0}{L^{eff}}\sqrt{\frac{F_1^2 + F_2^2}{B_1^2 + B_2^2}}\frac{P}{2\pi}\cos\left(\frac{2\pi t}{P} - \varphi_L\right)\Bigg|_{t_1}^{t_2}$$

$$\Rightarrow \frac{Q_L}{A} = \frac{\sqrt{2}}{4}\sqrt{\frac{F_1^2 + F_2^2}{B_1^2 + B_2^2}}\rho c_p L^{eff}\left(\Delta T\right)_0\cos\left(\frac{2\pi t}{P} - \varphi_L\right)\Bigg|_{t_1}^{t_2}$$

$$\Rightarrow \frac{Q_L}{A} = \frac{1}{2}\zeta_{\varepsilon,\delta}^{L}c_{area}^{eff}\left(\Delta T\right)_0\cos\left(\frac{2\pi t}{P} - \varphi_L\right)\Bigg|_{t_1}^{t_2} \tag{3. 39}$$

where $\zeta_{\varepsilon,\delta}^{L} = \dfrac{\sqrt{2}}{2}\sqrt{\dfrac{F_1^2 + F_2^2}{B_1^2 + B_2^2}}$ (3. 40)

which can be called **Inner Effective Heat Exchange Coefficient** for certain ε and δ.

The amount of heat stored in the PTMs from t_1 to t_2 can be got as

$$\frac{Q_{stor}}{A} = \int_{t_1}^{t_2}\left(q_0^{"} - q_L^{"}\right)dt = \int_{t_1}^{t_2} q_0^{"}dt - \int_{t_1}^{t_2} q_L^{"}dt = \frac{Q_0}{A} - \frac{Q_L}{A}$$

$$\Rightarrow \frac{Q_{stor}}{A} = \frac{\sqrt{2}}{4} c_{area}^{eff} \left(\Delta T\right)_0 \left. \frac{\left(B_1 D_2 - B_2 D_1 - B_1 F_2 + B_2 F_1\right)\cos\left(\frac{2\pi t}{P}\right) + \left(B_1 D_1 + B_2 D_2 - B_1 F_1 - B_2 F_2\right)\sin\left(\frac{2\pi t}{P}\right)}{B_1^{\,2} + B_2^{\,2}} \right|_{t_1}^{t_2}$$

$$\Rightarrow \frac{Q_{stor}}{A} = \frac{\sqrt{2}}{4} \sqrt{\frac{\left(D_1 - F_1\right)^2 + \left(D_2 - F_2\right)^2}{B_1^{\,2} + B_2^{\,2}}} c_{area}^{eff} \left(\Delta T\right)_0 \cos\left(\frac{2\pi t}{P} - \varphi_{stor}\right) \Bigg|_{t_1}^{t_2}$$

$$\Rightarrow \frac{Q_{stor}}{A} = \frac{1}{2} \zeta_{\varepsilon,\delta}^{stor} c_{area}^{eff} \left(\Delta T\right)_0 \cos\left(\frac{2\pi t}{P} - \varphi_{stor}\right) \Bigg|_{t_1}^{t_2} \tag{3. 41}$$

where $\zeta_{\varepsilon,\delta}^{stor} = \frac{\sqrt{2}}{2} \sqrt{\frac{\left(D_1 - F_1\right)^2 + \left(D_2 - F_2\right)^2}{B_1^{\,2} + B_2^{\,2}}}$ (3. 42)

which is called **Effective Heat Storage Coefficient** for certain ε and δ in this thesis;

and $\tan\varphi_{stor} = \frac{B_1 D_1 + B_2 D_2 - B_1 F_1 - B_2 F_2}{B_1 D_2 - B_2 D_1 - B_1 F_2 + B_2 F_1}$ (3. 43)

$$\Rightarrow t_{stor} = \frac{P}{2\pi}\varphi_{stor} = \frac{P}{2\pi}\tan^{-1}\left(\frac{B_1 D_1 + B_2 D_2 - B_1 F_1 - B_2 F_2}{B_1 D_2 - B_2 D_1 - B_1 F_2 + B_2 F_1}\right) \pm \frac{nP}{2} \tag{3. 44}$$

When $t = t_{stor}$, the amount of heat stored in or flowed out of the PTMs is maximum.

3.3 Results and discussions

3.3.1 Effective heat exchange coefficient

From Eqns. (3. 28) and (3. 30), we know that both t_0 and ζ^0 are functions of B_1, B_2, D_1 and D_2, which are all functions of δ and ε. Therefore, we can change values of these two parameters to see what will happen to t_0 and ζ^0.

From Eqn. (3. 8), δ should be a non-zero finite value. From Eqn. (3. 11), when

$h \to \infty$, $\varepsilon \to \infty$ and the B.C. of the third kind reduces to that of the first kind; when $h \to 0$, $\varepsilon \to 0$ and the B.C. of the third kind reduces to that of the second kind.

From Eqn. (3. 28), for certain ε and δ, when $q_0^{"} = 0$, the time t_0 is

$$t_0 = \frac{P}{2\pi}\tan^{-1}\left(\frac{\varepsilon^2\left[e^{4\delta} - 2e^{2\delta}\sin(2\delta) - 1\right] + 2\varepsilon\left[e^{4\delta} - 2e^{2\delta}\cos(2\delta) + 1\right] + 2\left[e^{4\delta} + 2e^{2\delta}\sin(2\delta) - 1\right]}{-\varepsilon^2\left[e^{4\delta} + 2e^{2\delta}\sin(2\delta) - 1\right] - 2\varepsilon\left[e^{4\delta} + 2e^{2\delta}\cos(2\delta) + 1\right] - 2\left[e^{4\delta} - 2e^{2\delta}\sin(2\delta) - 1\right]}\right) \pm \frac{nP}{2} \quad (3.\ 45)$$

From Eqn. (3. 29), the net heat gain/loss at the left surfaces in one period is

$$Q_{0\,max\,\text{3rd B.C.}} = \zeta^0_{\varepsilon,\delta} A c^{eff}_{area} \left(\Delta T\right)_0 \quad (3.\ 46)$$

where $$\zeta^0_{\varepsilon,\delta} = \sqrt{\frac{\varepsilon^2\left[e^{4\delta} + 2e^{2\delta}\cos(2\delta) + 1\right] + 2\varepsilon\left[e^{4\delta} - 2e^{2\delta}\sin(2\delta) - 1\right] + 2\left[e^{4\delta} - 2e^{2\delta}\cos(2\delta) + 1\right]}{\varepsilon^2\left[e^{4\delta} - 2e^{2\delta}\cos(2\delta) + 1\right] + 2\varepsilon\left[e^{4\delta} + 2e^{2\delta}\sin(2\delta) - 1\right] + 2\left[e^{4\delta} + 2e^{2\delta}\cos(2\delta) + 1\right]}} \quad (3.\ 47)$$

When $\varepsilon \to \infty$ (corresponding to the B.C. of the first kind),

$$t_{0\,\text{1st B.C.}} = \frac{P}{2\pi}\tan^{-1}\left(\frac{e^{4\delta} - 2e^{2\delta}\sin(2\delta) - 1}{-e^{4\delta} - 2e^{2\delta}\sin(2\delta) + 1}\right) \pm \frac{nP}{2} \quad (3.\ 48)$$

and $$Q_{0\,max\,\text{1st B.C.}} = \zeta^0_{\infty,\delta} A c^{eff}_{area} \left(\Delta T\right)_0 \quad (3.\ 49)$$

where $$\zeta^0_{\infty,\delta} = \sqrt{\frac{e^{4\delta} + 2e^{2\delta}\cos(2\delta) + 1}{e^{4\delta} - 2e^{2\delta}\cos(2\delta) + 1}} \quad (3.\ 50)$$

When $\varepsilon \to 0$ (corresponding to the B.C. of the second kind),

$$t_{0\,\text{2nd B.C.}} = \frac{P}{2\pi}\tan^{-1}\left(\frac{e^{4\delta} + 2e^{2\delta}\sin(2\delta) - 1}{-e^{4\delta} + 2e^{2\delta}\sin(2\delta) + 1}\right) \pm \frac{nP}{2} \quad (3.\ 51)$$

and $$Q_{0\,max\,\text{2nd B.C.}} = \zeta^0_{0,\delta} A c^{eff}_{area} \left(\Delta T\right)_0 \quad (3.\ 52)$$

where $$\zeta^0_{0,\delta} = \sqrt{\frac{e^{4\delta} - 2e^{2\delta}\cos(2\delta) + 1}{e^{4\delta} + 2e^{2\delta}\cos(2\delta) + 1}} \quad (3.\ 53)$$

t_0 and ζ^0 against δ of different ε are plotted in Figure 3.1 and Figure 3.2. Note: Since the t_0 and ζ^0 bands are very narrow as ε increases from 6 to positive infinite, curves are not shown in these two figures.

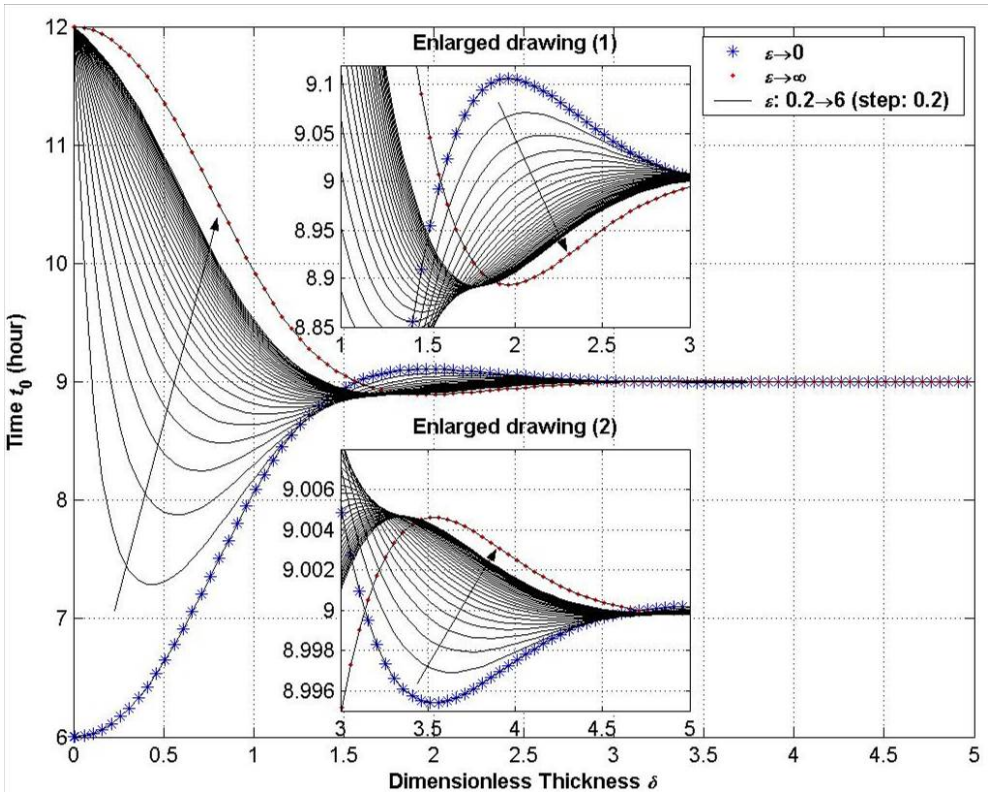

Figure 3.1—The time t_0 when $q_0^{"}$=0

From Figure 3.1, it is clear that

(a) As δ increases from zero, t_0 first decreases from $P/2=12$ hour to a trough, and then increases to a crest, and then decreases to another trough, …, just as a wave. The "wave" decreases so fast that after the first progression (around $\delta \approx 3$), it keeps nearly at $3P/8=9$ hour (the maximum difference is less than one minute);

(b) As ε decreases from positive infinite to zero, all the corresponding troughs and crests move "ahead" (to a smaller δ). When $\varepsilon \to 0$, the first trough moves so ahead that it decreases from $P/2$ to $P/4$ immediately at around $\delta = 0$;

(c) It can be considered that the line of $\varepsilon \to \infty$ (which is corresponding to the B.C. of the first kind) and the line of $\varepsilon = 0$ (which is corresponding to the B.C. of the second kind) are symmetrical relative to the straight line $t = 3P/8$.

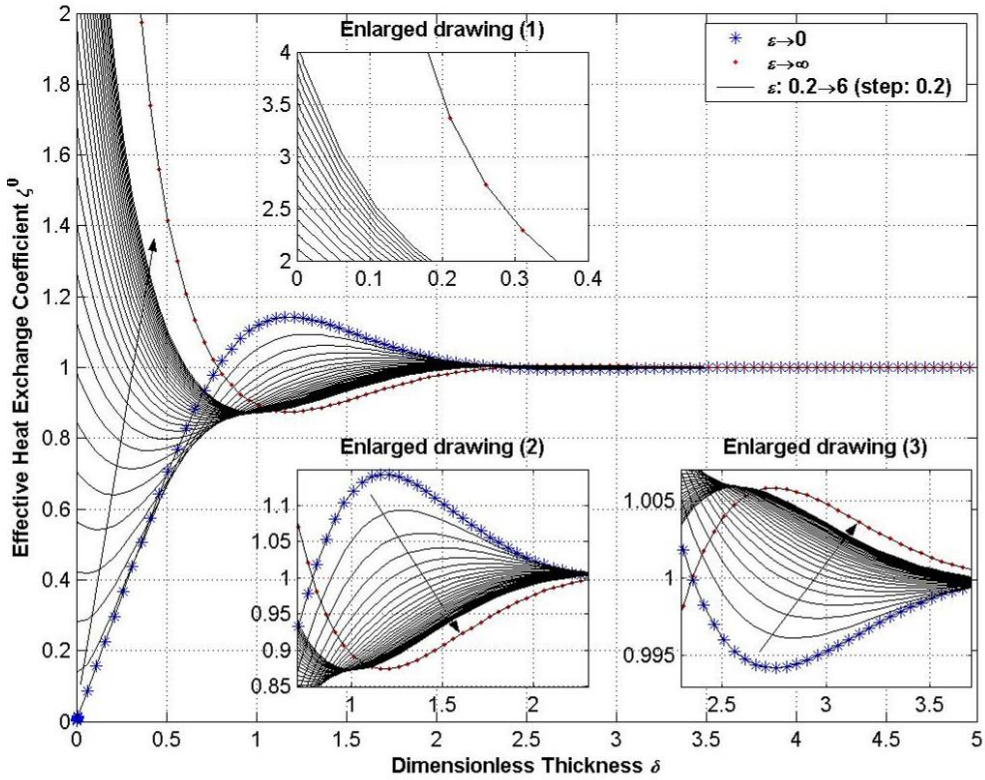

Figure 3.2—The effective heat exchange coefficient ζ^0

From Figure 3.2, we know that

(a) If δ is very small and ε is large ($\delta \le 0.2$ and $\varepsilon \ge 3$), ζ^0 can be very large (more than 2, even reach 10);

(b) When ε is small ($0.2 < \varepsilon < 2$), as δ increases from zero, ζ^0 decreases first, and then increases, and then decreases … also like a wave. After the first progression of the "wave" (around $\delta \approx 2$), ζ^0 keeps nearly at a constant 1, which is equal to the value of the semi-infinite PTM discussed in Chapter 2;

(c) When ε is smaller ($\varepsilon \le 0.5$), as δ increases from zero, ζ^0 increases first, and then decreases, and then increases… After the first progression, ζ^0 also keeps nearly at the constant 1.

(d) For $\varepsilon \to 0$, ζ^0 has the maximum value 1.143 when $\delta = \delta^* = 1.1825$. Since the right surfaces are insulated in this case, all the heat transferred into the left surfaces is stored in the PTMs. We call this maximum value of ζ^0 as **Optimal Effective Thermal Mass Coefficient** and denote it as ζ_0^*; the corresponding δ^* is called **Optimal Dimensionless Thickness** and

$$L^* = \delta^* L^{eff} \Big/ \sqrt{2} \tag{3. 54}$$

is called **Optimal Thermal Mass Thickness**. Therefore, the maximum amount of heat stored in PTMs with $L = L^*$ can be gotten as

$$Q_{max}\left(L^*\right) = \zeta_0^* A c_{area}^{eff} \left(\Delta T\right)_0 \tag{3. 55}$$

When P = 24 hours, based on the properties listed in Table 2, values of L^* and $\zeta_0^* c_{area}^{eff}$ of some common building materials are figured out and listed in Table 8, at the end of this chapter.

3.3.2 Effective heat storage coefficient

From Eqn. (3. 41), the maximum heat stored in the PTMs in one period is

$$Q_{stor\ max} = \zeta_{\varepsilon,\delta}^{stor} A c_{area}^{eff} \left(\Delta T\right)_0 \tag{3. 56}$$

From Eqn. (3. 44), when the amount of heat stored in or flowed out of the PTMs is maximum, the time t_{stor} is

$$t_{stor} = \frac{P}{2\pi} \tan^{-1}\left(\frac{B_1 D_1 + B_2 D_2 - B_1 F_1 - B_2 F_2}{B_1 D_2 - B_2 D_1 - B_1 F_2 + B_2 F_1}\right) \pm \frac{nP}{2} \tag{3. 57}$$

t_{stor} and ζ^{stor} against δ of different ε are plotted are plotted in Figure 3.3 and

Figure 3.4. Note: Since the t_{stor} and ζ^{stor} bands are very narrow as ε increases from 6 to positive infinite, curves are not shown in these two figures.

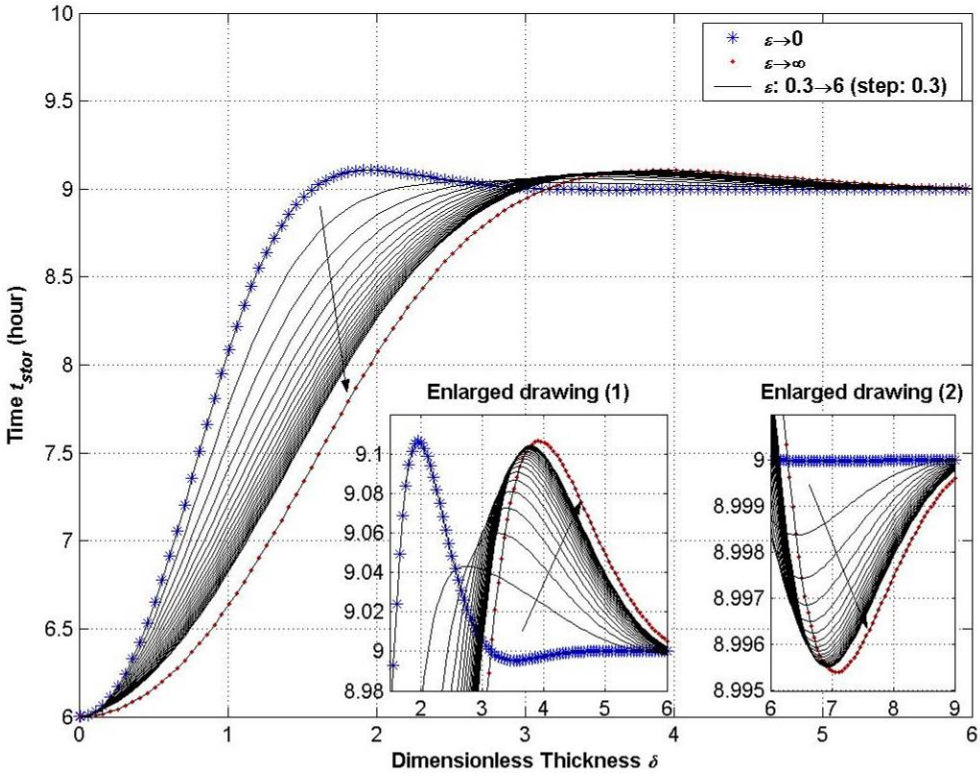

Figure 3.3—The time t_{stor} when Q_{stor} is maximum

Curves in the above figure are very different from that in Figure 3.1 except the line when $\varepsilon \to 0$. As δ increases from zero, all curves increase first, rather than decrease like curves in Figure 3.1. However, except this difference, the trends are the same as δ keeping on increasing. Finally, all curves keep nearly at $3P/8 = 9$ hour.

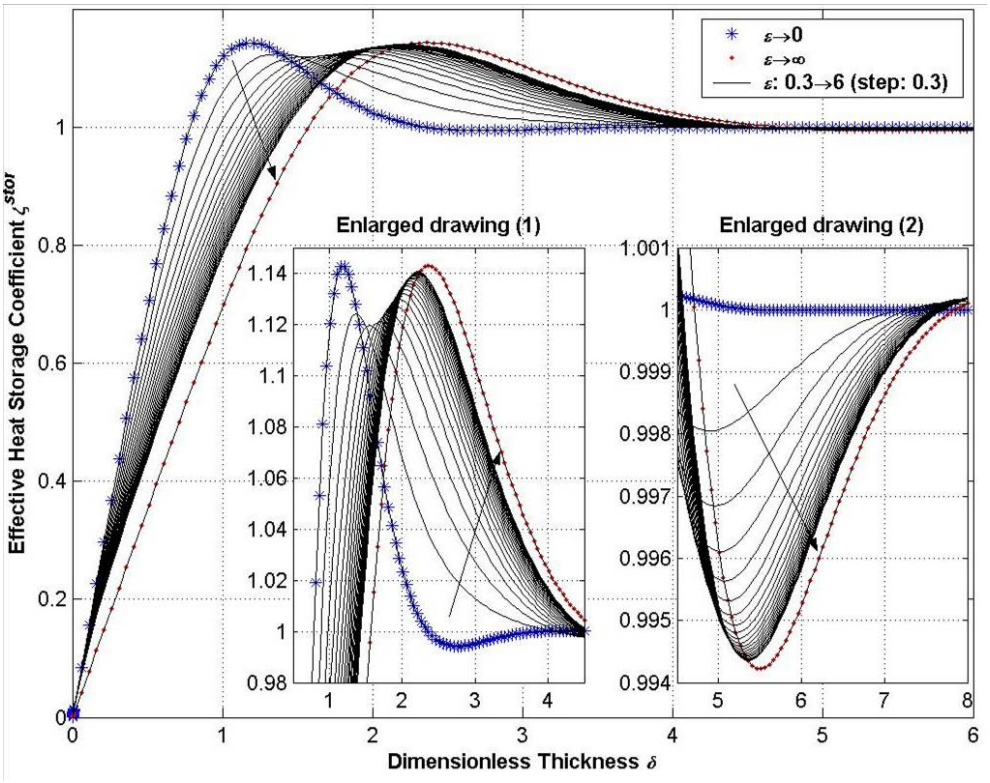

Figure 3.4—The effective heat storage coefficient ζ^{stor}

Unlike ζ^0 in Figure 3.2, ζ^{stor} in Figure 3.4 increases almost linearly when δ is small ($\delta \le 1$ for small ε PTMs to $\delta \le 2$ for large ε PTMs), which means that the amount of stored heat energy increases almost linearly with the thickness of the PTM when δ is not large. Generally, it is natural to try to thicken a PTM to make it be a better thermal mass. However, from Figure 3.4, we realize that if we continue to thicken the PTM after a certain thickness, the heat stored in the PTM actually decreases a little. That's because previously stored energy is trying to flow out of the PTM and interfaces the influent heat.

3.4 Examples

3.4.1 Wood wall and concrete wall

Now, we can answer the question brought forward at the end of Chapter 1: Why is a wood wall of twice or three-times, even four-times the thickness of a concrete wall still a much poorer thermal mass than the concrete wall?

First, we take the building as a whole, which means that we just consider the heat exchange at the outside surface of the wall. In this case, what we need to consider is the effective heat exchange coefficient ζ^0 of wood and concrete. From Table 8, we know that $\varepsilon_{wood} \approx 4.621$ and $\varepsilon_{concrete} \approx 0.718$ (normal-weight concrete), and then from Eqn. (3.6), we can draw out ζ^0 of wood and concrete against δ, as shown in Figure 3.5.

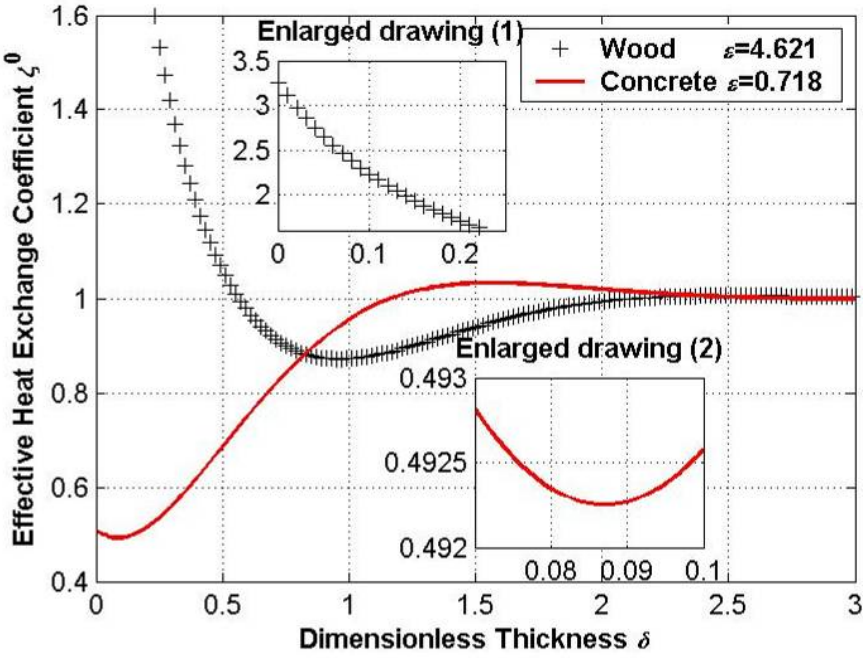

Figure 3.5—ζ^0 of wood and concrete against δ

From the figure above, we can find that the minimum ζ^0 of a concrete wall is about 0.4923 (at $\delta \approx 0.087$ and the thickness of the concrete wall is $L = \delta L^{eff} / \sqrt{2} \approx 1.46$ cm). In Table 3, it is shown that the effective area specific heat of wood and normal-weight concrete are $c^{eff}_{area\ \mathrm{wood}} = 68.207$ kJ/m^2·K and $c^{eff}_{area\ \mathrm{concrete}} = 439.037$ kJ/m^2·K, respectively. When the environment conditions are the same, according to the definition of ζ^0, if a wood wall is as good thermal mass as a normal-weight concrete wall, the effective heat exchange coefficient ratio of the wood wall and the concrete wall should be $Ratio = \dfrac{c^{eff}_{area\ \mathrm{concrete}}}{c^{eff}_{area\ \mathrm{wood}}} = \dfrac{439.037}{68.207} \approx 6.437$. Therefore, the minimum ζ^0 of the wood wall should be about $6.437 \times 0.4923 \approx 3.169$ (Note: $\zeta^0 \equiv \dfrac{Q_{0max}}{Ac^{eff}_{area}\left(\Delta T\right)_0}$), and then from the curve of wood in the figure above, the dimensionless thickness δ of the wood wall should be less than 0.01, which means that the wood wall should be less than 1 millimeters. It is not applied for such a thin wood wall, and thus we may suppose that a wood wall will never as good thermal mass as a normal-weight concrete wall if we take the building as a whole.

If building envelope is separated from the outside and inside environments, what we need to consider is the effective heat storage coefficient ζ^{stor} of wood and concrete. From Eqn. (3. 8), we can draw out ζ^{stor} of wood and concrete against δ, as shown in Figure 3.6.

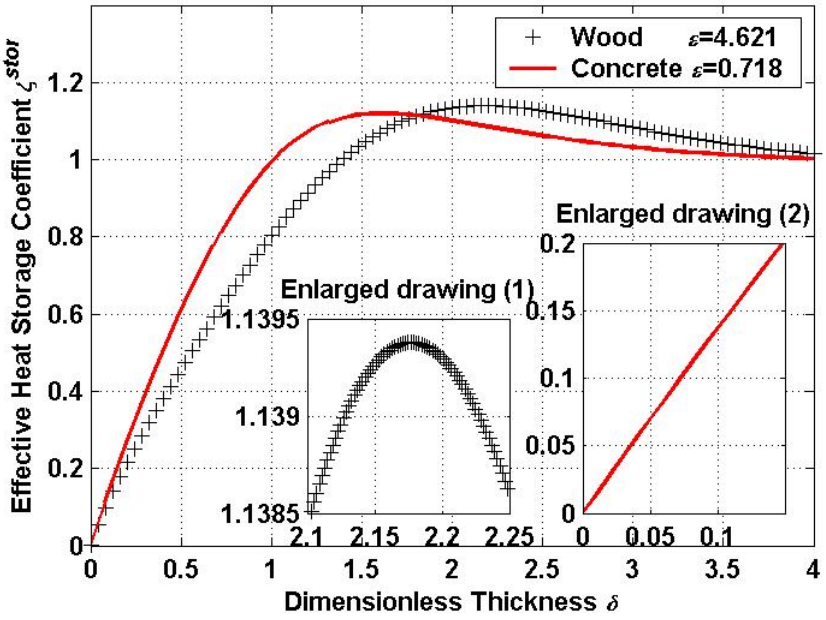

Figure 3.6—ζ^{stor} of wood and concrete against δ

From the figure above, we know that the maximum value of ζ^{stor} of a wood wall is about 1.1394 (at $\delta \approx 2.18$ and the wood wall thickness is $L = \delta L^{eff} / \sqrt{2} \approx 14.9$ cm). Therefore, the maximum value of ζ^{stor} of the concrete wall should be about $1.1394 \div 6.437 \approx 0.177$, and then from the curve of concrete in the figure above, the effective thickness δ of the concrete wall should be less than 0.13, which means that the concrete wall should be less than 2.2 cm (0.866 inch). That is to say, if a normal-weight concrete wall is thicker than 2.2 cm, there is no wood wall as good thermal mass as the concrete wall.

The maximum amounts of heat exchange between the environment and a wood/concrete wall with the increase of thickness are listed in Table 4. The maximum amounts of heat stored in a wood/concrete wall with the increase of thickness are listed in Table 5.

Table 4—Maximum heat exchange between wood/concrete walls and the environment (h = 8.1037 W/m^2·K)

Thickness L [m]	$Q_{0\,max\,\text{3rd B.C.}} / A(\Delta T)_0$ [kJ/m^2·K]	
	Wood	Concrete
0.025	85.4	219.1
0.05	61.8	245.1
0.1	63.7	327.9
0.15	68.3	400.2
0.2	68.5	440.6
0.25	68.2	453.1
0.3	68.2	451.4
0.35	68.2	446.0
0.4	68.2	441.7

Table 5—Maximum heat storage of wood/concrete walls (h = 8.1037 W/m^2·K)

Thickness L [m]	$Q_{\text{stor}\,max\,\text{3rd B.C.}} / A(\Delta T)_0$ [kJ/m^2·K]	
	Wood	Concrete
0.025	24.1	87.8
0.05	42.7	167.9
0.1	70.0	307.1
0.15	77.7	410.1
0.2	74.4	468.9
0.25	70.4	490.1
0.3	68.4	489.7
0.35	67.8	480.8
0.4	67.9	470.4

To sum up, if a concrete wall is thicker than a certain thickness (2.2 cm in this thesis), no matter how thicker than the concrete wall, a wood wall is always a poor thermal mass than the concrete wall when subjected to periodic heating and cooling.

3.4.2 Internal PTMs

It is shown that, in Figure 3.2 and Figure 3.4, the two curves when $\varepsilon \to 0$ (corresponding to the B.C. of the second kind) are the same. The case when $\varepsilon \to 0$ is important in our lives. Dynamic heat transfer of all internal PTMs can be boiled down to this case.

Consider a PTM (for example, an internal wall or a wood board of a desk) of thickness 2L such that the other two dimensions are very large compared to the thickness 2L, as shown in Figure 3.7, in a building. If it is allowed to float, the inside air

temperature can be treated as a sinusoidal variations $T_{inside\,air} = (\Delta T)_{in} \sin(2\pi t/P) + T_{m\,in}$, where $(\Delta T)_{in}$ and $T_{m\,in}$ are the peak amplitude and the mean value of the inside air temperature. Therefore, the thermal wave at the surfaces of the PTM is also sinusoidal with the same mean value $T_m = T_{m\,in}$, although its peak amplitude will be smaller than that of the inside air temperature, because of the convection heat transfer at the PTM surfaces. The amount of the amplitude decrease depends on thermo-physical properties of the PTM, the temperature variations of the inside air, and of course the heat transfer coefficient *h* (in this thesis, *h* = 8.1037 W/m^2·K is chosen for natural convection heat transfer inside of buildings; however, actually, it is always changing in certain extent). The convective effect at the outside surfaces can be obtained as follows.

From Eqn. (3. 52) or Eqn. (3. 56), for internal PTMs,

$$Q_{max} = \zeta_{0,\delta} A c_{area}^{eff} (\Delta T)_0 \tag{3. 58}$$

where $\zeta_{0,\delta}$ can be found out, in Figure 3.2 or Figure 3.4, on the line of $\varepsilon \to 0$. Then a **Virtual Average Heat Flux** can be gotten as

$$q_{av}^{"} = \frac{Q_{max}}{P/2} = A \frac{(\Delta T)_0}{\frac{P/2}{\zeta_{0,\delta} c_{area}^{eff}}} = A \frac{(\Delta T)_0}{R_{eff}} \tag{3. 59}$$

where $R_{eff} = \dfrac{P/2}{\zeta_{0,\delta} c_{area}^{eff}}$ (3. 60)

which can be called **Effective Thermal Resistance** [m^2·K/W] of thermal mass. Note: For $\varepsilon \to 0$, $\zeta_{0,\delta} = \zeta_{0,\delta}^{0} = \zeta_{0,\delta}^{stor}$; for other cases, $\zeta_{0,\delta} = \zeta_{0,\delta}^{0}$. And also note: when heat flows into PTM, $q_{av}^{"}$ is positive, and when heat flows out of PTM, $q_{av}^{"}$ is negative. Since the

effective thermal resistance of thermal mass and the convective thermal resistance are in series, the smaller the effective thermal resistance of thermal mass, the bigger the convective effect. Therefore, the maximum effect of convection occurs when $\delta = \delta^* = 1.1825$ and $\zeta_0^* = 1.143$, and the minimum effective thermal resistance for a certain material is

$$R_{eff}^* = \frac{P/2}{\zeta_0^* c_{area}^{eff}} \tag{3. 61}$$

At last, the minimum peak amplitude of T_0 can be gotten as

$$(\Delta T)_{0min} = (\Delta T)_{in} \frac{R_{eff}^*}{1/h + R_{eff}^*} \tag{3. 62}$$

Values of R_{eff}^* and the proportion of $(\Delta T)_{0min}/(\Delta T)_{in}$ of some common building materials are listed in Table 8, at the end of this chapter. For most common building materials, the convective effect can not be neglected, since the heat transfer coefficient *h* in buildings is small. However, at the outside of buildings, it may be neglected since the heat transfer coefficient is much bigger.

After knowing $(\Delta T)_0$, we can go back to the heat transfer problem of internal PTMs. The G.D.E. Eqn. (2. 1) or (2. 5) and the B.C. Eqn. (2. 3) or (2. 7) are still applied for the problem. Since the thermal as well as the geometric symmetries of the problem, the heat flux at the virtual mid-surfaces of the PTMs must be zero and thus the other B.C. should be changed into

$$-k\left(\frac{\partial T}{\partial x}\right)_L = q_L'' = 0 \quad \text{and} \quad \left(\frac{\partial \theta}{\partial x}\right)_L = 0 \tag{3. 63}$$

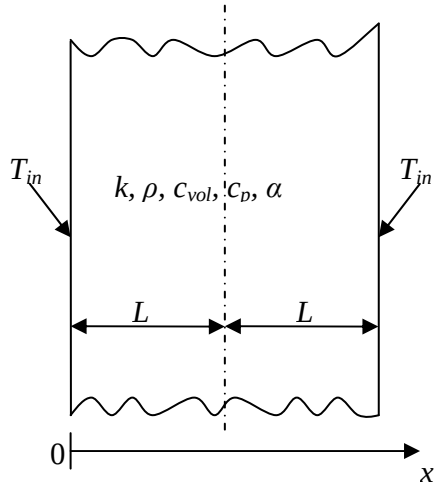

Figure 3.7—PTM of thickness 2*L*

Just consider the left half part of the PTMs. As discussed before, in this case, the effective heat exchange coefficient and the effective heat storage coefficient for the same δ are identical. Here we call it effective thermal mass coefficient and denote it as ζ_0. The curve of ζ_0 against δ ($\delta = \sqrt{2}L/L^{eff}$) is reproduced and shown in Figure 3.8. We also know that, when $\delta = \delta^* = 1.1825$, $\zeta_0^* = 1.143$ is called the optimal effective thermal mass coefficient, which is the maximum value on the curve. This particular point is shown in Figure 3.8, too.

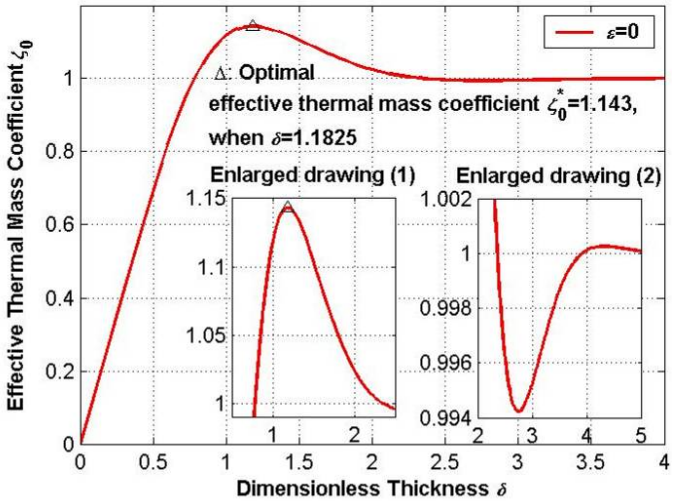

Figure 3.8—The effective thermal mass coefficient ζ_0

The temperature distributions of PTMs with different δ for $\varepsilon \to 0$ are shown in Figure 3.9.

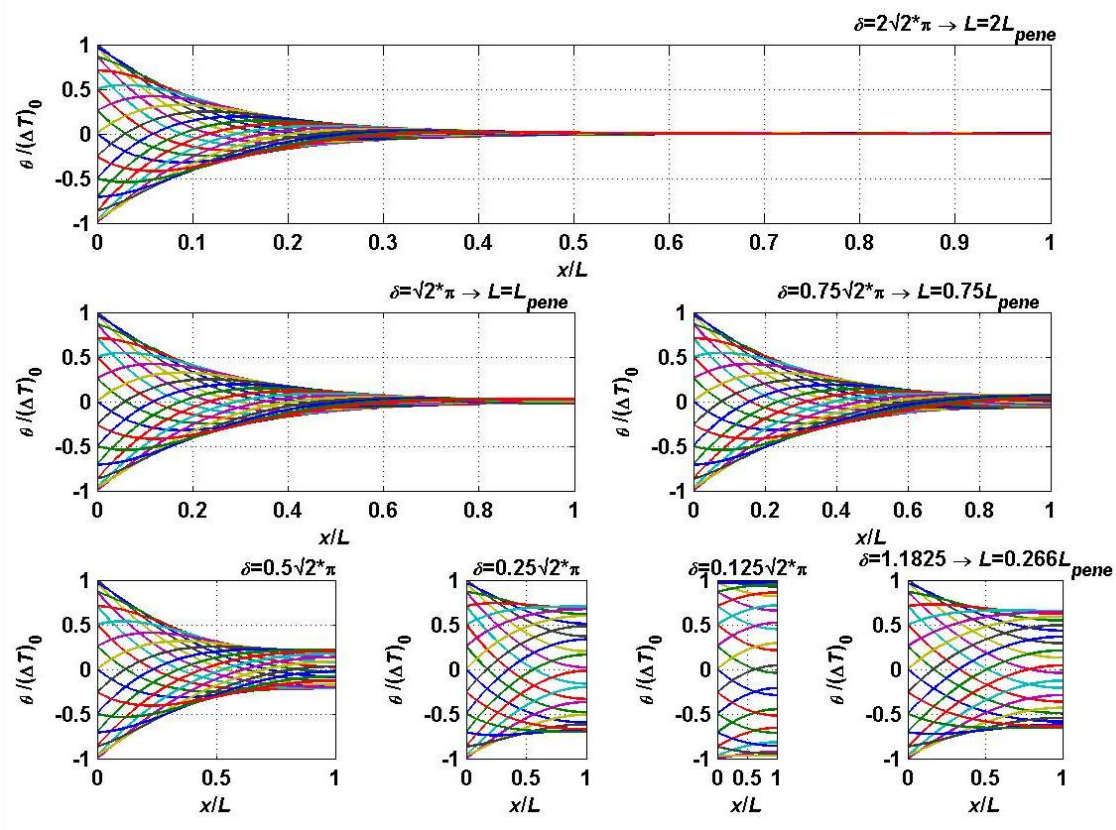

Figure 3.9—Temperature distributions of internal PTMs with different δ

Define a **dimensionless heat flux** as

$$q''_{dim} = \frac{L^{eff}}{\sqrt{2}k\left(\Delta T\right)_0} q'' \tag{3. 64}$$

and dimensionless heat fluxes at the surfaces of PTMs with different δ are shown in Figure 3.10.

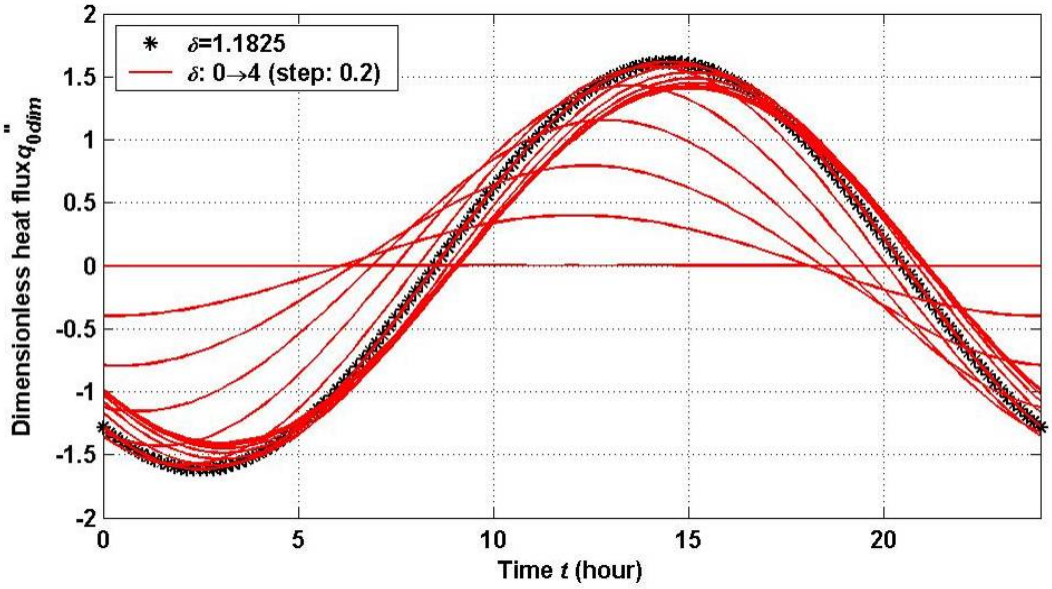

Figure 3.10—Surface heat fluxes of internal PTMs with different δ

For any curve in Figure 3.10, the enclosed area below the curve and above the straight line $q_0'' = 0$, is the amount of net heat energy absorbed, in one period, by the internal PTM with the corresponding δ; and the enclosed area above the curve and below the straight line $q_0'' = 0$, is the amount of net heat energy released. Of course, since the amount of absorbed and released heat is equivalent in one period, these two areas are equal for the same curve. Thus we can just consider the upper half, which is shown in Figure 3.11.

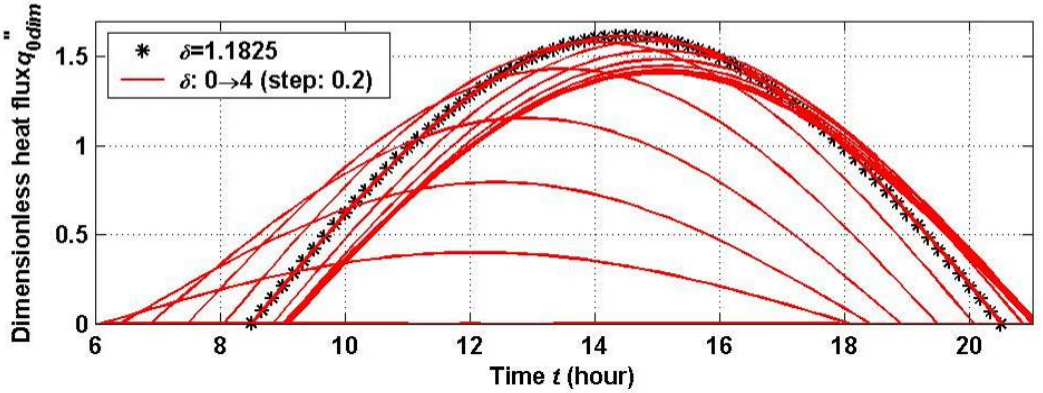

Figure 3.11—Surface heat fluxes of internal PTMs with different δ (upper half)

In the figure above, since periods are the same, curve with bigger amplitude encloses larger area. We can find that the curve with $\delta = \delta^* = 1.1825$ encloses the largest area, which intuitively confirms the optimal thermal mass thickness $L^* = \delta^* L_{pene} / \sqrt{2}\pi = \delta^* L^{eff} / \sqrt{2}$. Of course, for internal PTMs, the optimal thickness is $2L^* \approx 0.5323 L_{pene} \approx 1.6723 L^{eff}$.

The maximum amounts of heat stored in half part of internal wood/concrete walls are listed in Table 6.

Table 6—Maximum heat storage of internal wood/concrete walls (half part)

h = 0

Half thickness $L/2$ [m]	$Q_{0\,max\ \text{2nd B.C.}} / A(\Delta T)_0$ [kJ/m^2·K]	
	Wood	Concrete
0.025	35.0	92.2
0.05	65.0	184.0
0.081	78.0	
0.1	75.8	355.4
0.15	68.8	470.3
0.199		501.8
0.2	67.9	501.8
0.25	68.2	485.8
0.3	68.2	462.3
0.35	68.2	446.3
0.4	68.2	438.7

From the table above, it is clear that

(a) When an internal wood wall is thicker than 0.162 m, it can store less heat energy, which means that it becomes a worse thermal mass;

(b) When an internal concrete wall is thicker than 0.398 m, it becomes a worse thermal mass.

3.5 Summary

In this chapter, when $T_{inside\ air} = T_m$, the dynamic heat transfer of finite-thickness PTMs is investigated. The temperature distribution function in finite-thickness PTMs is deduced. The heat exchange between the PTMs and the environment (the effective heat exchange coefficient and the inner effective heat exchange coefficient) and the heat storage of the PTMs (the effective heat storage coefficient) are developed. The time when the outside surface heat flux is equal to zero and the time when the amount of heat stored in or flowed out of the PTMs is maximum are obtained. It shows that all the coefficients and times vary as a decaying wave with the increase of the thickness. Later, two examples are given. The first one shows that a wood wall is always a poor thermal mass than a concrete wall larger than 2.2 cm; and the second one gives the optimal thickness of internal PTMs.

Some definitions of properties, parameters and coefficients are listed in table 7.

Table 7—Definitions of properties, parameters and coefficients

Parameters	**Symbols or definitions**	**Units**	**Eqns.**
Dimensionless thickness	$\delta \equiv \frac{\sqrt{2}L}{L^{eff}} = \frac{\sqrt{2}\pi L}{L_{pene}} = \sqrt{\frac{\pi}{\alpha P}}L$	dimensionless	(3. 9)
Dynamic Biot number	$\varepsilon \equiv \frac{hL^{eff}}{\sqrt{2}k} = \frac{hL_{pene}}{\sqrt{2}\pi k}$	dimensionless	(3. 12)
Effective heat exchange coefficient	$\zeta_{\varepsilon,\delta}^{0} \equiv \frac{Q_{0\,max}}{Ac_{area}^{eff}\left(\Delta T\right)_0}$	dimensionless	(2. 33) (3. 31) (3. 32)
Inner effective heat exchange coefficient	$\zeta_{\varepsilon,\delta}^{L} \equiv \frac{Q_{L\,max}}{Ac_{area}^{eff}\left(\Delta T\right)_0}$	dimensionless	(3. 41) (3. 42)
Effective heat storage coefficient	$\zeta_{\varepsilon,\delta}^{stor} = \frac{Q_{stor\,max}}{Ac_{area}^{eff}\left(\Delta T\right)_0}$	dimensionless	(3. 43) (3. 44)
Optimal thermal mass thickness	$L^{*} = \frac{\delta^{*}L^{eff}}{\sqrt{2}}$	m	(3. 54)
Optimal effective thermal mass coefficient	$\zeta_0^{*} = \frac{Q_{max}(L^{*})}{Ac_{area}^{eff}\left(\Delta T\right)_0} \approx 1.143$	dimensionless	(3. 55)
Optimal dimensionless thickness	$\delta^{*} = 1.1825$	dimensionless	①
Effective thermal resistance	$R_{eff} = \frac{P/2}{\zeta_{0,\delta}^{0}c_{area}^{eff}}$	m^2·K/W	(3. 60)
Optimal effective thermal resistance	$R_{eff}^{*} = \frac{P/2}{\zeta_0^{*}c_{area}^{eff}}$	m^2·K/W	(3. 61)
Dimensionless heat flux	$q_{dim}^{"} = \frac{L^{eff}}{\sqrt{2}k\left(\Delta T\right)_0}q^{"}$	dimensionless	(3. 64)

① The optimal dimensionless thickness is shown in Figure 3.8.

Values of ε, L^*, $\zeta_0^* c_{area}^{eff}$, R_{eff}^* and the proportion of $(\Delta T)_{0min}/(\Delta T)_{in}$ of some common building materials are listed in Table 8.

Table 8—Values of some definitions of different building materials

Material	Dynamic Biot number ② $\varepsilon = \frac{hL^{eff}}{\sqrt{2}k}$	Optimal thermal mass thickness $L^* = \frac{\delta^* L^{eff}}{\sqrt{2}}$	$\zeta_0^* c_{area}^{eff}$	Optimal effective thermal resistance $R_{eff}^* = \frac{P/2}{\zeta_0^* c_{area}^{eff}}$	$\frac{(\Delta T)_{0min}}{(\Delta T)_{in}} = \frac{R_{eff}^*}{\frac{1}{h} + R_{eff}^*}$ ②
	dimensionless	[m]	[kJ/m^2·K]	[m^2·K/W]	dimensionless
Wood	4.621	0.0809	77.96	0.5541	81.79 %
Normal-weight Concrete	0.718	0.1990	501.82	0.0861	41.10 %
Building Brick	1.183	0.1260	304.57	0.1418	53.47 %
Structural lightweight concrete	1.418	0.1262	254.15	0.1670	57.51 %
Insulating lightweight concrete	5.184	0.1059	69.49	0.6217	83.44 %
Face brick	0.817	0.1550	440.81	0.0980	44.26 %
Mineral fiber (loosefill)	74.194	0.5197	4.86	8.8889	98.63 %
Glass fiberboard (resin binder)	15.863	0.0972	22.71	1.8981	93.90 %
Expanded polystyrene	38.285	0.1620	9.41	4.5909	97.38 %
Gypsum board	3.600	0.0840	100.08	0.4317	77.77 %
Steel	0.101	0.6657	3577.05	0.0121	8.93 %

② In the dynamic Biot number and the equation, h = 8.1037 W/m^2·K.

Chapter 4: Dynamic Heat Transfer of Finite-thickness PTMs When $T_{inside\ air} \neq T_m$

In the preceding two chapters, analytical method is used to solve the dynamic heat transfer problems of the semi-infinite PTM and finite-thickness PTMs when the inside air temperature is equal to the mean value of outside surface temperature ($T_{inside\ air} = T_m$). However, "the vast majority of problems encountered in practice cannot be solved analytically as they usually involve irregular geometries with mathematically inconvenient mixed boundary conditions. In such cases, numerical and/or graphical methods often provide the answer." ([34]: page 283) In this chapter, the finite-difference method [34], one of the most frequently used numerical methods, will be used to solve the dynamic heat transfer problem of finite-thickness PTMs when $T_{inside\ air} \neq T_m$.

4.1 Principle of the finite-difference method

The core idea of the finite-difference method is replacing the G.D.E. and B.C.s by algebraic equations. Three kinds of approximate expressions exist for the first derivative of $T(x)$ at a point x_j, as shown in Figure 4.1:

The forward-difference form: $$\left.\frac{dT}{dx}\right|_{x_j} \approx \frac{T_{j+1} - T_j}{\Delta x} \qquad (4.1)$$

The backward-difference form: $$\left.\frac{dT}{dx}\right|_{x_j} \approx \frac{T_j - T_{j-1}}{\Delta x} \qquad (4.2)$$

The central-difference form: $\left.\frac{dT}{dx}\right|_{x_j} \approx \frac{T_{j+1}-T_{j-1}}{2\Delta x}$ (4. 3)

where $j = 0,1,2,\mathrm{L}\ , J$.

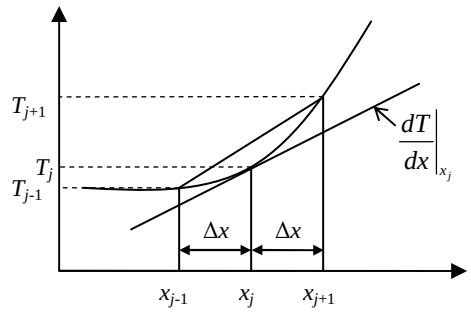

Figure 4.1—Finite-difference approximation of derivatives

The finite-difference approximation for the second derivative of $T(x)$ in central-difference form is

$$\left.\frac{d^2T}{dx^2}\right|_{x_j} \approx \frac{\left.(dT/dx)\right|_{x_j+\Delta x/2} - \left.(dT/dx)\right|_{x_j-\Delta x/2}}{\Delta x} \approx \frac{\left(T_{j+1}-T_j\right)/\Delta x - \left(T_j-T_{j-1}\right)/\Delta x}{\left(\Delta x\right)^2}$$

$$\Rightarrow \left.\frac{d^2T}{dx^2}\right|_{x_j} \approx \frac{T_{j+1}-2T_j+T_{j-1}}{\left(\Delta x\right)^2} \qquad (4.\ 4)$$

In dynamic heat transfer processes, it is time dependant. By dividing x and t domains into small intervals of Δx and Δt, the finite-difference approximation for the second-order partial derivative at point x_j and time t_n is represented as

$$\left.\frac{\partial^2T}{\partial x^2}\right|_{x_j,t_n} \approx \frac{T_{j+1}^n-2T_j^n+T_{j-1}^n}{\left(\Delta x\right)^2} \qquad (4.\ 5)$$

where $n = 0,1,2,\mathrm{L}\ , N$.

The time derivative may also be approximated in terms of forward-, backward- or central-difference form. By using the forward-difference form, the G.D.E. (2. 1) can be written as

$$\frac{T_{j+1}^n - 2T_j^n + T_{j-1}^n}{(\Delta x)^2} = \frac{1}{\alpha}\frac{T_j^{n+1} - T_j^n}{\Delta t} \tag{4. 6}$$

which can be rearranged as

$$\text{G.D.E.} \quad T_j^{n+1} = \left(1 - \frac{2}{\beta}\right)T_j^n + \frac{1}{\beta}\left(T_{j+1}^n + T_{j-1}^n\right) \tag{4. 7}$$

$$\text{where} \quad \beta = \frac{(\Delta x)^2}{\alpha \Delta t} \tag{4. 8}$$

which should be not smaller than 2 in order to get stable solutions. ([34]: page 298)

The B.C. (2. 3) can be used directly in numerical calculation:

$$\text{B.C.} \qquad T_0^n = (\Delta T)_0 \sin\left(\frac{2\pi}{P}t_n\right) + T_m \tag{4. 9}$$

By the finite-difference approximation, the B.C. (3. 3) should be written as

$$-k\frac{T_J^{n+1} - T_{J-1}^{n+1}}{\Delta x} = h\left(T_J^{n+1} - T_{inside\ air}\right) \tag{4. 10}$$

which can be rearranged as

$$\text{B.C.} \qquad T_J^{n+1} = \frac{1}{1+\gamma}\left(T_{J-1}^{n+1} + \gamma T_{inside\ air}\right) \tag{4. 11}$$

$$\text{where} \quad \gamma = \frac{h\Delta x}{k} \tag{4. 12}$$

and to get stable solutions, it must have

$$\gamma \le \beta/2 - 1 \tag{4. 13}$$

Using Eqns. (4. 7), (4. 9) and (4. 11), we can solve the dynamic heat transfer problem completely by numerical method. Since k and α are materials' thermo-physical properties, which should be known in numerical calculation, we should take certain materials as examples. In this thesis, we will again take wood and concrete walls for example.

4.2 Development of approximated analytical solutions

Suppose that the environment is represented by summer (July), Las Vegas, NV. The outdoor air temperature (also be approximated as the wall-outside-surface temperature) is a sinusoidal function with a period of 24 hours, and the highest and lowest temperatures are 105 °F (40.56 °C/313.71 K) and 78 °F (25.56 °C/298.71 K), respectively. That is,

$$T_{out} = 7.5\sin\left(\frac{2\pi t}{P}\right) + 33.06(\text{°C}) = 7.5\sin\left(\frac{2\pi t}{P}\right) + 306.21(\text{K}) \tag{4. 14}$$

The indoor air temperature is kept at 75 °F (23.89 °C/297.04 K) by a heat pump or air-conditioning unit, that is, $T_{inside\ air} = 297.04\ \text{K}$.

Before using numerical method to solving the problem when $T_{inside\ air} \neq T_m$, check the accuracy of the method first. When $T_{inside\ air} = T_m = 306.21\,\text{K}$, numerical calculation results of wood walls are shown in Figure 4.2. In the figure,

$$\zeta^{0in} \equiv \frac{Q_{0in\ max}}{Ac_{area}^{eff}\left(\Delta T\right)_0} \tag{4. 15}$$

$$\zeta^{0out} \equiv \frac{Q_{0out\ max}}{Ac_{area}^{eff}\left(\Delta T\right)_0} \tag{4. 16}$$

$$\zeta^{Lin} \equiv \frac{Q_{Lin\ max}}{Ac_{area}^{eff}\left(\Delta T\right)_0} \tag{4. 17}$$

$$\zeta^{Lout} \equiv \frac{Q_{Lout\ max}}{Ac_{area}^{eff}\left(\Delta T\right)_0} \tag{4. 18}$$

and $\zeta^{steady} \equiv \frac{Q_{steady\ max}}{Ac_{area}^{eff}\left(\Delta T\right)_0}$ (4. 19)

where $Q_{0in\ max}$ — the total heat flowed into the wall outside surfaces in one period;

$Q_{0out\ max}$ — the total heat flowed out of the wall outside surfaces in one period;

$Q_{Lin\ max}$ — the total heat flowed into the wall inside surfaces in one period;

$Q_{Lout\ max}$ — the total heat flowed out of the wall inside surfaces in one period;

and $Q_{steady\ max}$ — the total heat flowed through the walls in one period if we assume that $T_0 = T_m$.

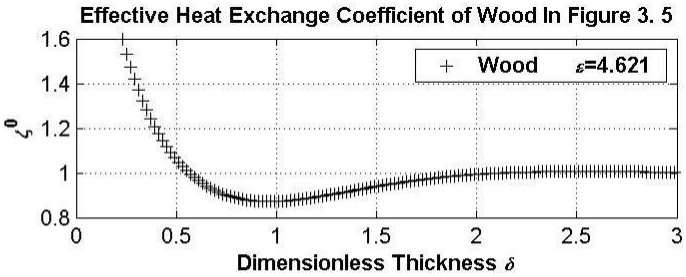

Analytical results (also shown in Figure 3.5)

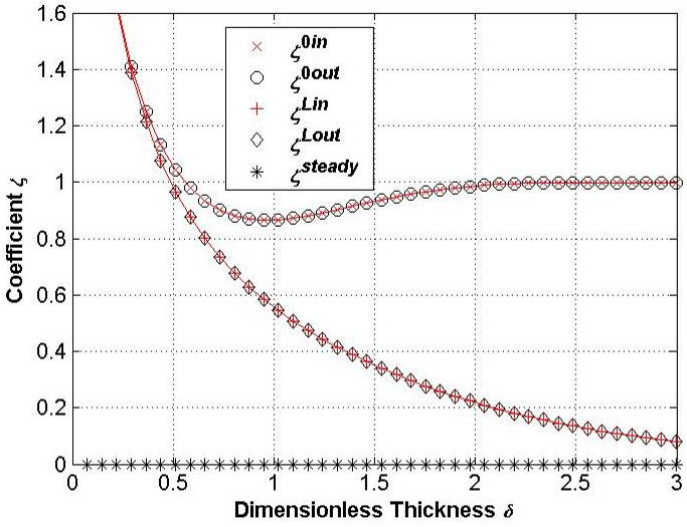

Numerical results

Figure 4.2—Coefficients of wood walls when $T_{inside\ air} = T_m$

In the Figure above, the curve of ζ^{0in} and the curve of ζ^{0out} are overlapped, that is, $Q_{0in\ max} = Q_{0out\ max}$; and comparing with the ζ^0 curve of wood in Figure 3.5, we can conclude that the numerical method has a great accuracy to solve the problem.

Now let $T_{inside\,air} = 297.04$ K. From the numerical calculation, the temperature distributions (where $\theta(x,t) = T(x,t) - T_m$) of wood walls and concrete walls are plotted in Figure 4.3 and 4.4, respectively.

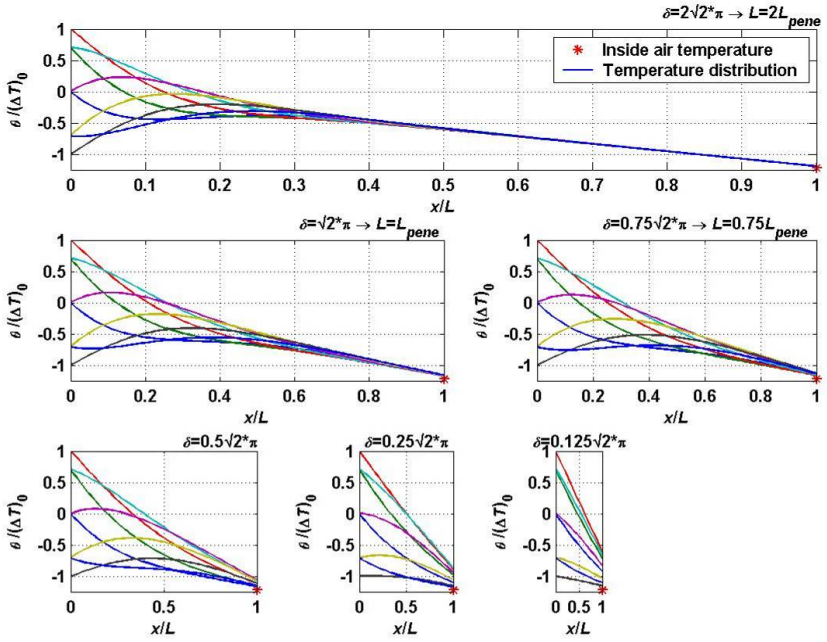

Figure 4.3—Temperature distributions of wood walls (July, Las Vegas, NV)

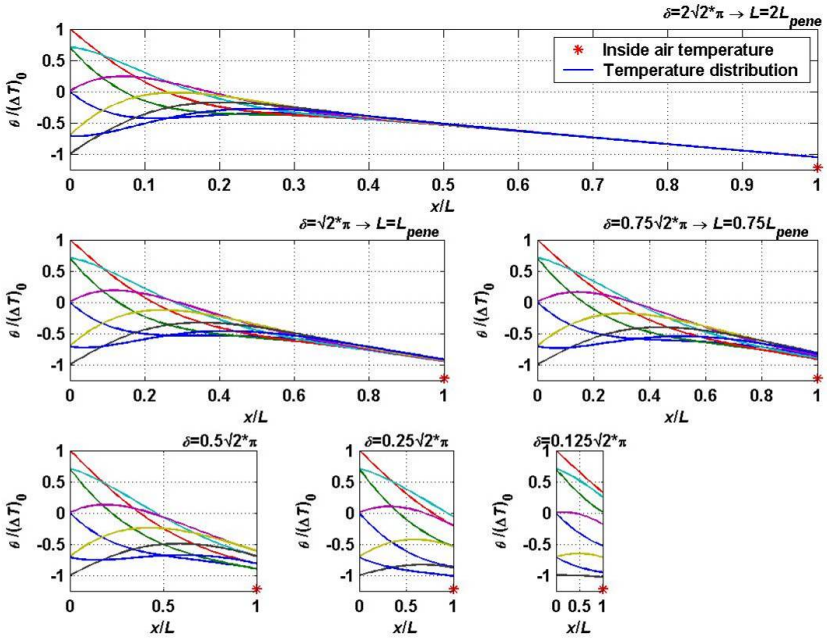

Figure 4.4—Temperature distributions of concrete walls (July, Las Vegas, NV)

Based on numerical results, approximated functions should be developed to describe the dynamic heat transfer problem, since numerical calculation needs too much time.

By using the principle of superposition, a liner part should be added because of the temperature difference of the wall outside surface and the inside air. From Eqn. (3. 17), the simplest form of the temperature distribution (Form I) is

$$\theta_{\mathrm{I}}(x,t)=(\Delta T)_0\frac{A_2B_1-A_1B_2}{B_1^2+B_2^2}+(T_{inside\,air}-T_m)\frac{x}{L} \tag{4. 20}$$

and plot it in Figure 4.5.

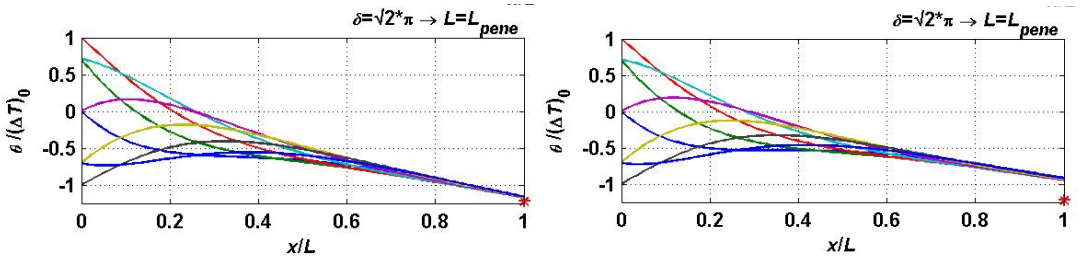

Numerical results (also shown in Figure 4.3 and Figure 4.4)

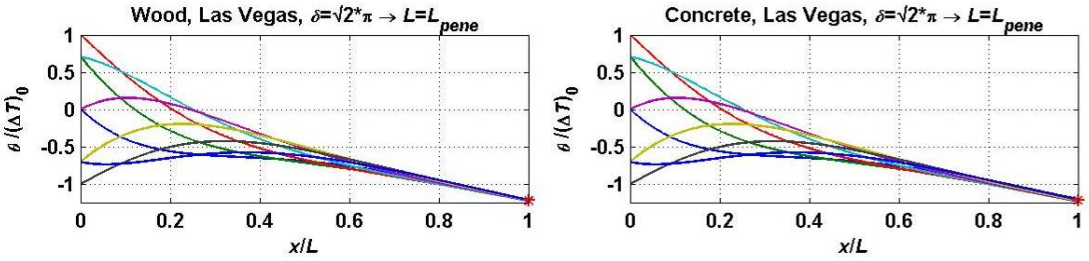

Analytical results of Form I

Figure 4.5—Temperature distributions of Form I (July, Las Vegas, NV)

Comparing the figures above, it is easy to find that Form I does not work well.

Now change $T_{inside\,air}$ in Eqn. (4.20) to $T_{m\,L}$, which is the mean value of the wall-inside-surface temperature, and the temperature distribution becomes

$$\theta(x,t)=(\Delta T)_0\frac{A_2B_1-A_1B_2}{B_1^2+B_2^2}+(T_{m\,L}-T_m)\frac{x}{L} \tag{4. 21}$$

The problem here is how we can get T_{mL}.

Treat T_0 as T_m and it becomes a steady-state heat transfer problem. And then

$$\frac{T_{mL}-T_m}{T_{inside\,air}-T_m}=\frac{L/k}{L/k+1/h}=\frac{1}{1+k/hL}=\frac{1}{1+\sqrt{2}k/\delta hL^{eff}}=\frac{1}{1+1/\delta\varepsilon} \tag{4. 22}$$

Let $T_\Delta = T_{inside\,air}-T_m$ (4. 23)

and then Eqn. (4. 21) can be rewritten as (Form II)

$$\theta_{\mathrm{II}}(x,t)=(\Delta T)_0\frac{A_2B_1-A_1B_2}{B_1^2+B_2^2}+\frac{T_\Delta}{1+1/\delta\varepsilon}\frac{\sqrt{2}x}{\delta L^{eff}} \tag{4. 24}$$

Let $\eta = T_\Delta/(\Delta T)_0$ (4. 25)

and then $\theta_{\mathrm{II}}(x,t)=(\Delta T)_0\left(\frac{A_2B_1-A_1B_2}{B_1^2+B_2^2}+\frac{\eta}{\delta+1/\varepsilon}\frac{\sqrt{2}x}{L^{eff}}\right)$ (4. 26)

In the case of Las Vegas, $\eta_{\text{Las Vegas}}=\frac{297.04\text{K}-306.21\text{K}}{7.5\text{K}}\approx -1.2227$.

The temperature distributions of Form II are plotted in Figure 4.6.

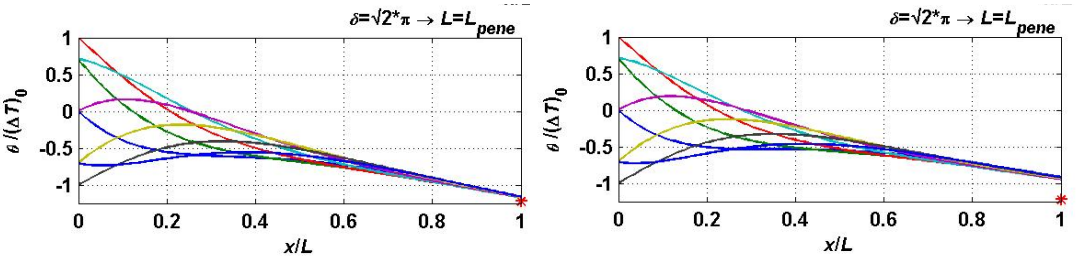

Numerical results (also shown in Figure 4.3 and Figure 4.4)

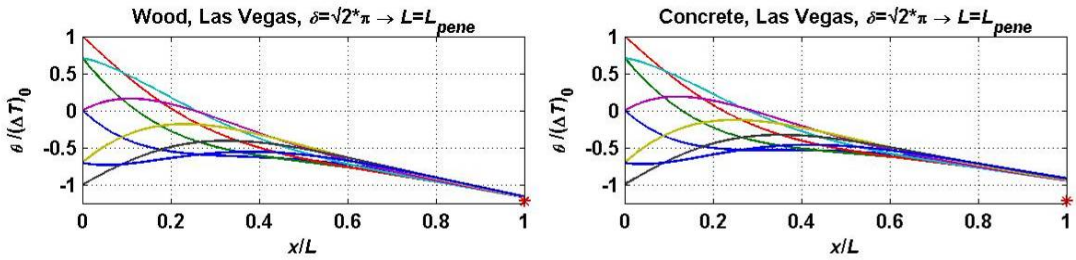

Analytical results of Form II

Figure 4.6—Temperature distributions of Form II (July, Las Vegas, NV)

Comparing the figures above, it looks that Form II works well.

There is also a Form III based on the discussion in Chapter 3:

$$\frac{T_{m\,L}-T_m}{T_{inside\,air}-T_m}=\frac{R_{eff}}{R_{eff}+1/h} \tag{4. 27}$$

$$\theta_{\mathrm{III}}(x,t)=(\Delta T)_0\left(\frac{A_2B_1-A_1B_2}{B_1^2+B_2^2}+\eta\frac{R_{eff}}{R_{eff}+1/h}\frac{\sqrt{2}x}{\delta L^{eff}}\right) \tag{4. 28}$$

where $R_{eff}=\dfrac{P/2}{\zeta_{0,\delta}^{0}c_{area}^{eff}}$.

Form III is too complex to be used. Therefore, we will check the accuracy of Form II by other parameters to see whether it is good enough to be used.

Take $\delta=\sqrt{2}\pi$ (which means that $L=L_{pene}$) for example, the time-dependent temperature variations at several points of the wood wall and that of the concrete wall are shown in Figure 4.7 and Figure 4.8, respectively.

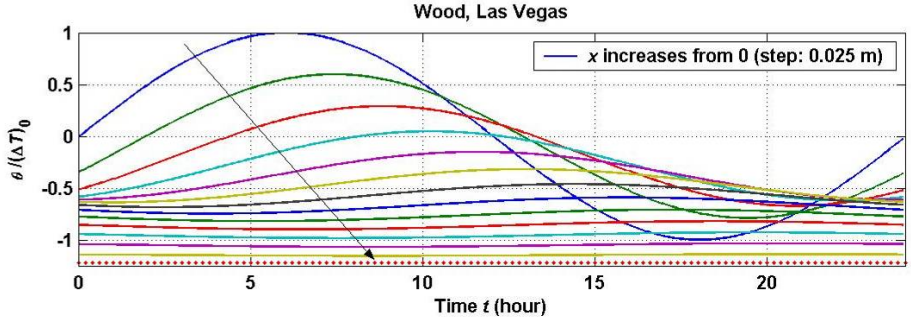

Numerical results

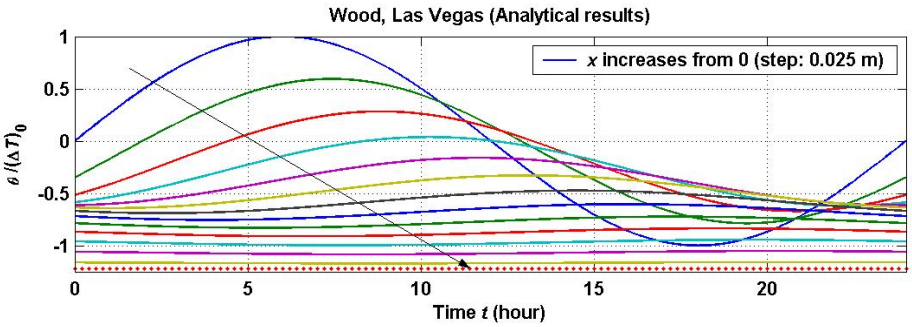

Analytical results

Figure 4.7—Temperature variations of the wood wall (July, Las Vegas, NV)

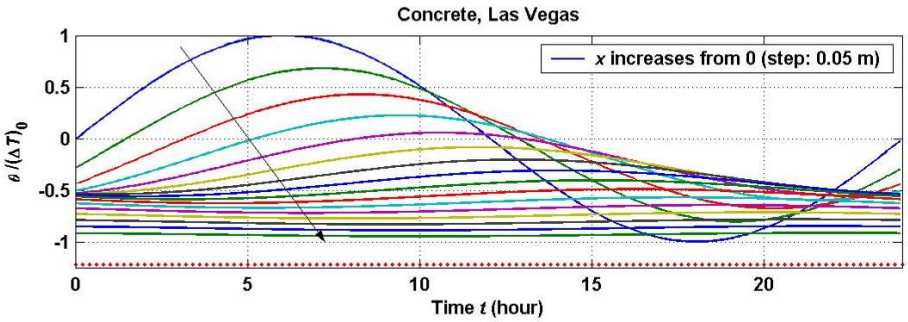

Numerical results

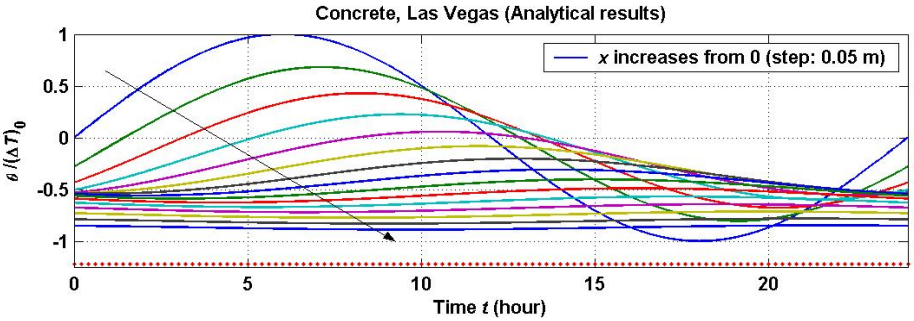

Analytical results

Figure 4.8—Temperature variations of the concrete wall (July, Las Vegas, NV)

From the temperature function of Form II, the heat flux can be gotten as

$$q^{"} = -k\frac{\partial \theta}{\partial x} = -k\left(\Delta T\right)_0\left[\frac{B_1\frac{\partial A_2}{\partial x} - B_2\frac{\partial A_1}{\partial x}}{B_1^2 + B_2^2} + \frac{\sqrt{2}\eta}{L^{eff}\left(\delta + 1/\varepsilon\right)}\right] \tag{4. 29}$$

When $x = 0$,

$$q_0^{"} = -\frac{\sqrt{2}k\left(\Delta T\right)_0}{L^{eff}}\left[\sqrt{\frac{D_1^2 + D_2^2}{B_1^2 + B_2^2}}\sin\left(\frac{2\pi t}{P} - \varphi_0\right) + \frac{\eta}{\delta + 1/\varepsilon}\right] \tag{4. 30}$$

and when $x = L$,

$$q_L^{"} = -\frac{\sqrt{2}k\left(\Delta T\right)_0}{L^{eff}}\left[\sqrt{\frac{F_1^2 + F_2^2}{B_1^2 + B_2^2}}\sin\left(\frac{2\pi t}{P} - \varphi_L\right) + \frac{\eta}{\delta + 1/\varepsilon}\right] \tag{4. 31}$$

The surface dimensionless heat fluxes ($q_{dim}^{"} = q^{"}L^{eff}\Big/\left[\sqrt{2}k\left(\Delta T\right)_0\right]$) of wood walls and that of concrete walls are plotted in Figure 4.9 and 4.10, respectively.

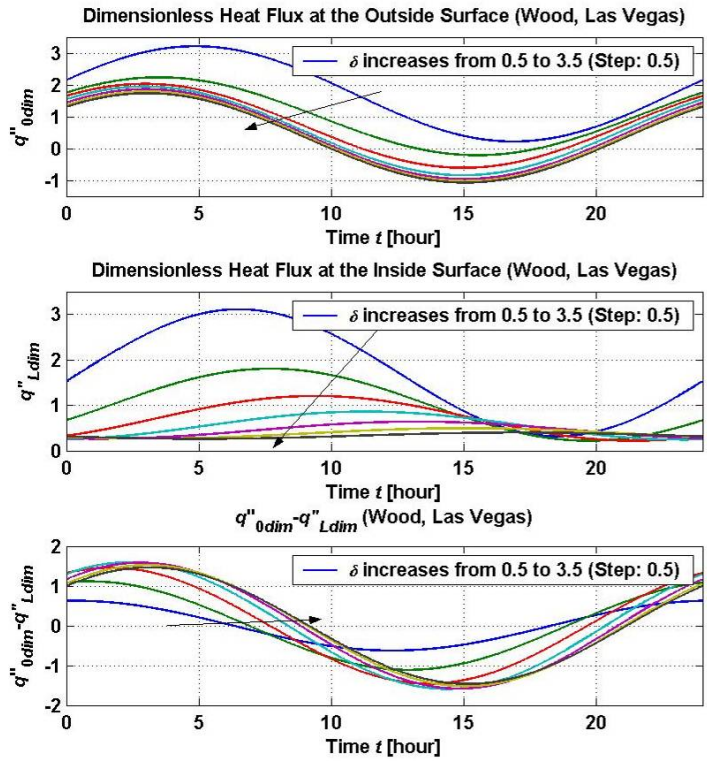

Numerical results

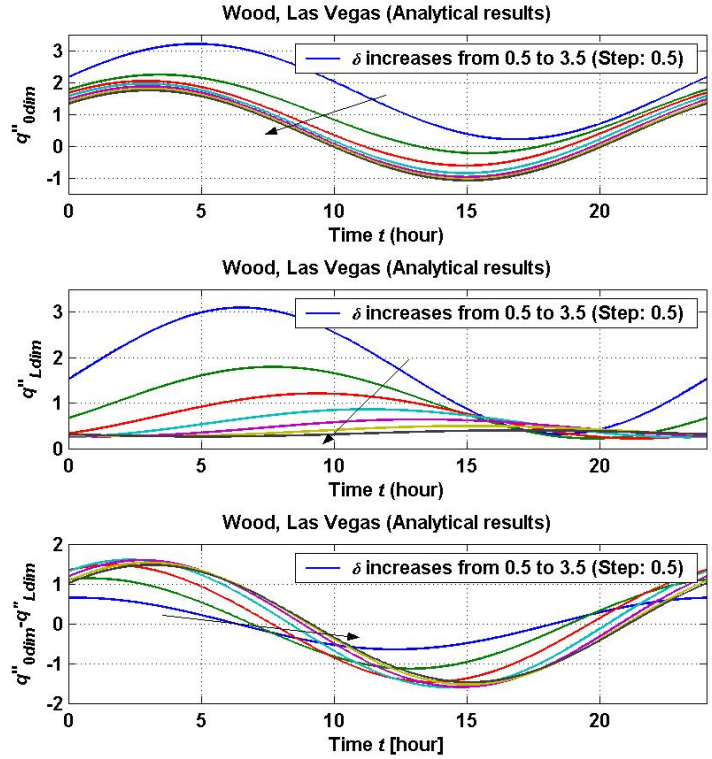

Analytical results

Figure 4.9—Surface heat fluxes of wood walls (July, Las Vegas, NV)

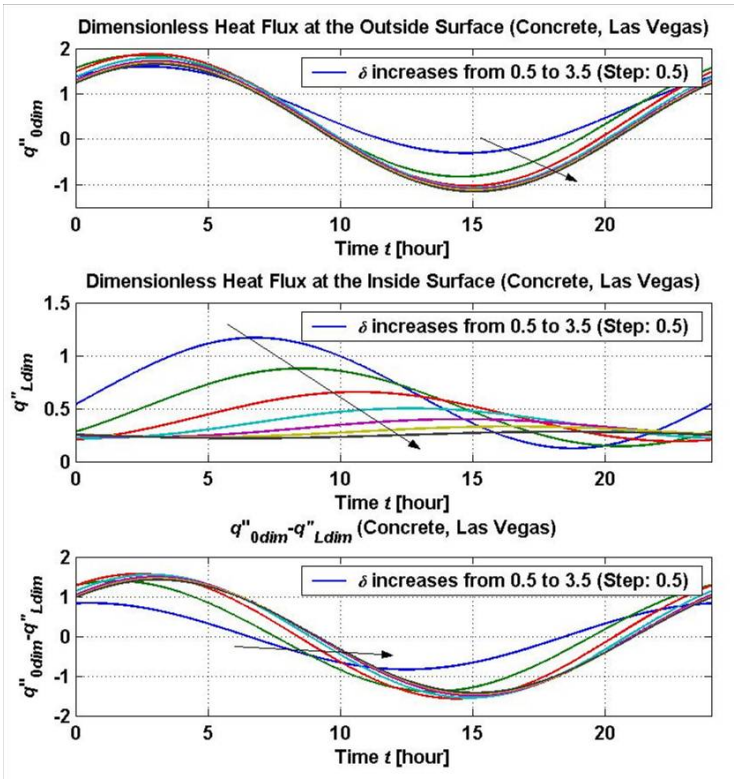

Numerical results

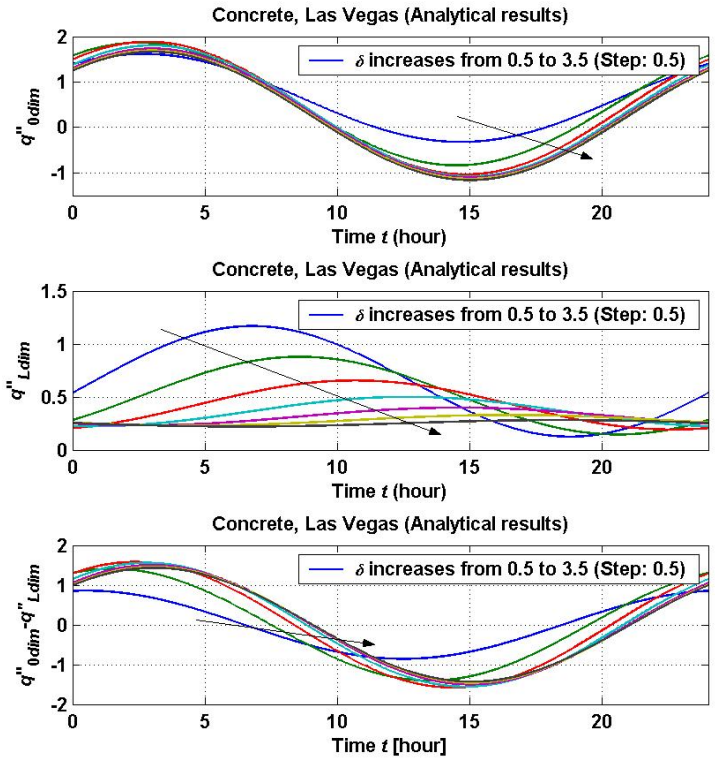

Analytical results

Figure 4.10—Surface heat fluxes of concrete walls (July, Las Vegas, NV)

The coefficients of wood walls and that of concrete walls are plotted in Figure 4.11 and Figure 4.12, respectively.

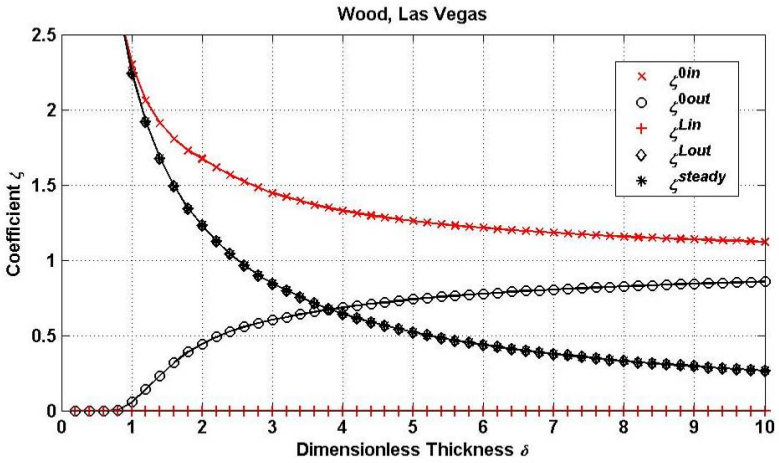

Numerical results

Note: the amount of heat flowed into the inside air is exactly equal to the steady value when δ is the same.

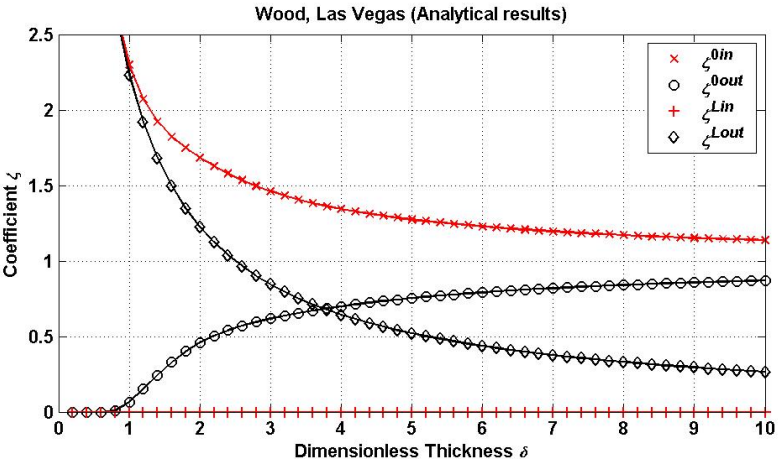

Analytical results

Figure 4.11—Coefficients of wood walls (July, Las Vegas, NV)

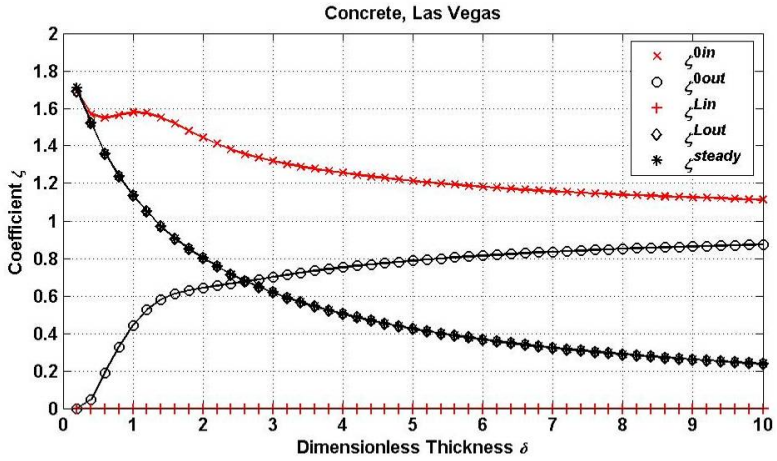

Numerical results

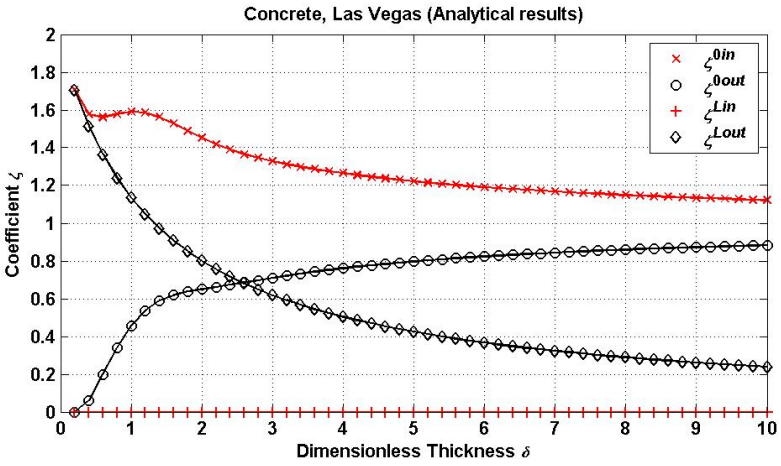

Analytical results

Figure 4.12—Coefficients of concrete walls (July, Las Vegas, NV)

All comparisons of the numerical calculation results and the results from Form II show that Form II has a great accuracy. Therefore, in this thesis, we will use Form II to get further analytical results.

4.3 Further analysis using Form II

4.3.1 The coefficients

From Eqn. (4. 30) and Eqn. (4. 31), we know that, for certain ε and δ, the effective

heat storage coefficient is the same, whether $T_{inside\,air} = T_m$ or $T_{inside\,air} \neq T_m$, since the linear parts ($\eta/(\delta + 1/\varepsilon)$) of $q_0^{"}$ and $q_L^{"}$ are cancelled out.

From the numerical results in Figure 4.11 and Figure 4.12, the amount of heat flowed into the inside air is exactly equal to the steady value when δ is the same ($\zeta^{Lout} = \zeta^{steady}$); that is to say, in these two cases, if we just concern the total heat flowed into the inside air, T_{out} can be treated as T_m, although T_{out} is a sinusoidal function. Four more numerical calculation cases are given as follows.

In Boston, MA, the highest and lowest average values of the outdoor air temperature, in January, are 36 °F (2.22 °C/275.37 K) and 22 °F (-5.56 °C/267.59 K), respectively. Treat the outdoor air temperature as a sinusoidal function:

$$T_{out} = 3.89 \sin\left(\frac{2\pi t}{P}\right) + 271.48(\mathrm{K}) \qquad (4.\ 32)$$

When the indoor air temperature is still kept at 75 °F (23.89 °C/297.04 K), the coefficients of wood walls and that of concrete walls are plotted in Figure 4.13 and Figure 4.14, respectively. (In these two cases, $\eta_{\mathrm{Boston}} \approx 6.5707$ and the indoor air temperature is higher than the highest value of the outdoor air temperature.)

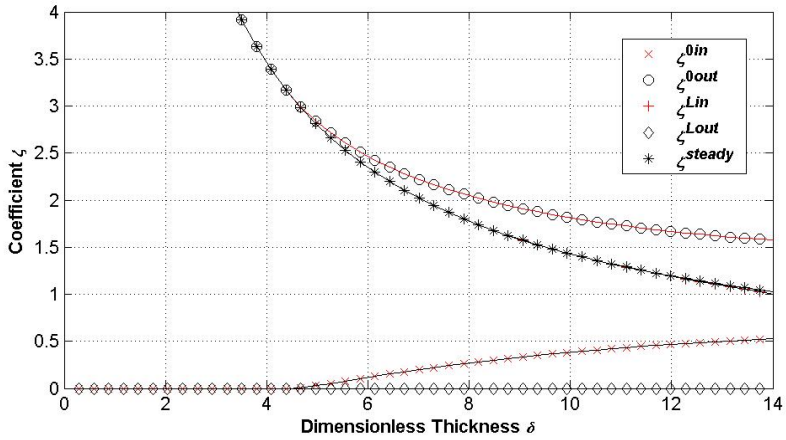

Figure 4.13—Coefficients of wood walls (January, Boston, MA)

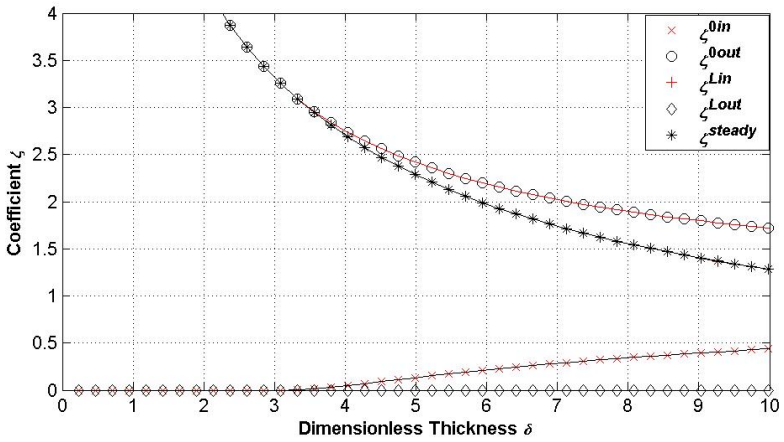

Figure 4.14—Coefficients of concrete walls (January, Boston, MA)

In the two cases above, the amount of heat flowed out of the inside air is exactly equal to the steady value when δ is the same ($\zeta^{Lin} = \zeta^{steady}$) and T_{out} can also be treated as T_m.

In August, the highest and lowest average values of the outdoor air temperature, in Denver, CO, are 86 °F (30 °C/303.15 K) and 52 °F (11.11 °C/284.26 K), respectively. Again, treat the outdoor air temperature as a sinusoidal function:

$$T_{out} = 9.45\sin\left(\frac{2\pi t}{P}\right) + 293.71(\mathrm{K}) \tag{4. 33}$$

When the indoor air temperature is still kept at 75 °F (23.89 °C/297.04 K), the

coefficients of wood walls and that of concrete walls are plotted in Figure 4.15 and Figure 4.16, respectively. (In these two cases, $\eta_{\text{Denver}} \approx 0.3524$ and the indoor air temperature is between the highest value and the lowest value of the outdoor air temperature.)

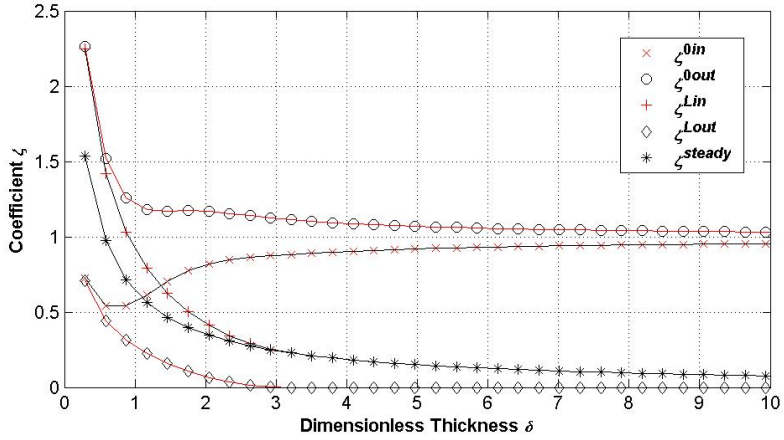

Figure 4.15—Coefficients of wood walls (August, Denver, CO)

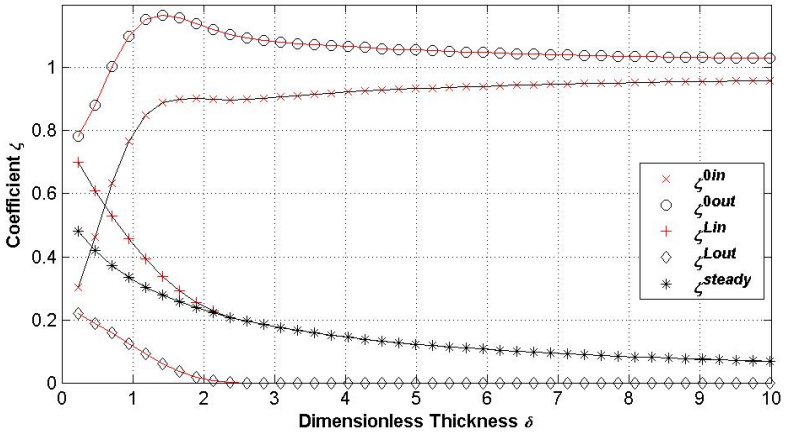

Figure 4.16—Coefficients of concrete walls (August, Denver, CO)

In the two cases above, when δ is large enough, the amount of heat flowed into the inside air becomes zero, and the amount of heat flowed out of the inside air is exactly equal to the steady value ($\zeta^{Lin} = \zeta^{steady}$), and T_{out} can be treated as T_m; however, when δ is small, these two kind of coefficients separate because of the variation of T_{out}, and in

such circumstances, T_{out} cannot be treated as T_m.

More calculations show that when $-1<\eta<1$, which means that the inside air temperature is between the maximum value and the minimum value of T_{out}, T_{out} cannot be treated as T_m if δ is small. Otherwise, the amount of heat flowed through walls just depends on the wall thermal resistance (L/k).

For wood and concrete walls, some curves of coefficients—ζ^{0in}, ζ^{0out}, ζ^{Lin} and ζ^{Lout}—against δ are plotted in Figure 4.17, Figure 4.18, Figure 4.19 and Figure 4.20. Note: $\eta<0$ means that $T_{inside\ air}<T_m$; $\eta<(-1)$ means that $T_{inside\ air}$ is lower than the lowest value of the outside surface temperature; $\eta>0$ means that $T_{inside\ air}>T_m$; $\eta>1$ means that $T_{inside\ air}$ is higher than the highest value of the outside surface temperature.

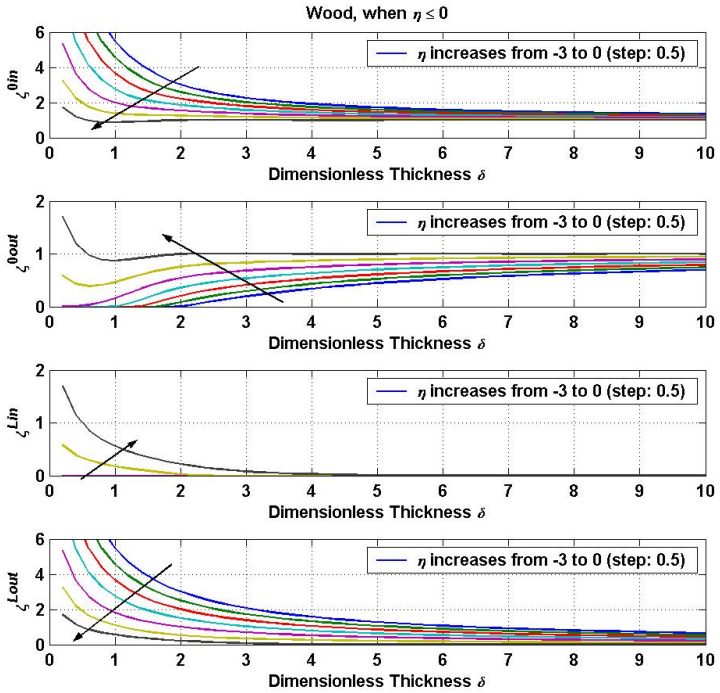

Figure 4.17—Coefficients of wood walls when $\eta \leq 0$

ζ^{0in}: As η increases, ζ^{0in} decreases when δ is the same; for certain η, ζ^{0in} decreases as δ increases and the decrease velocity becomes smaller when δ is larger;

when δ is large, ζ^{0in} trends to a constant value near 1 (a little larger than 1, except when $\eta = 0$); however, when η is close to zero and is δ small, ζ^{0in} decreases first and increases a little later, which phenomena was discussed in previous chapters when $\eta = 0$.

ζ^{0out}: As η increases, ζ^{0out} increases when δ is the same; when $\eta \le (-1)$, for certain η, ζ^{0out} increases from zero to near 1 (a little smaller than 1) as δ increases; when $-1 < \eta \le 0$, ζ^{0out} decreases first and increases a little later, then trends to a constant value near 1.

ζ^{Lin}: when $\eta \le (-1)$, $\zeta^{Lin} = 0$; when $-1 < \eta \le 0$, for certain η, ζ^{Lin} decreases as δ increases and finally becomes zero when δ is large enough.

ζ^{Lout}: As η increases, ζ^{Lout} decreases when δ is the same; for certain η, ζ^{Lout} decreases as δ increases and the decrease velocity becomes smaller when δ is larger; when δ is large, ζ^{0in} trends to a constant value near zero (a little larger than zero).

For $\eta = 0$, $\zeta^{0in} = \zeta^{0out}$ and $\zeta^{Lin} = \zeta^{Lout}$ when δ is the same. For certain η and δ, $\zeta^{0in} + \zeta^{Lin} = \zeta^{0out} + \zeta^{Lout}$, which means that in one period, the net heat stored is zero.

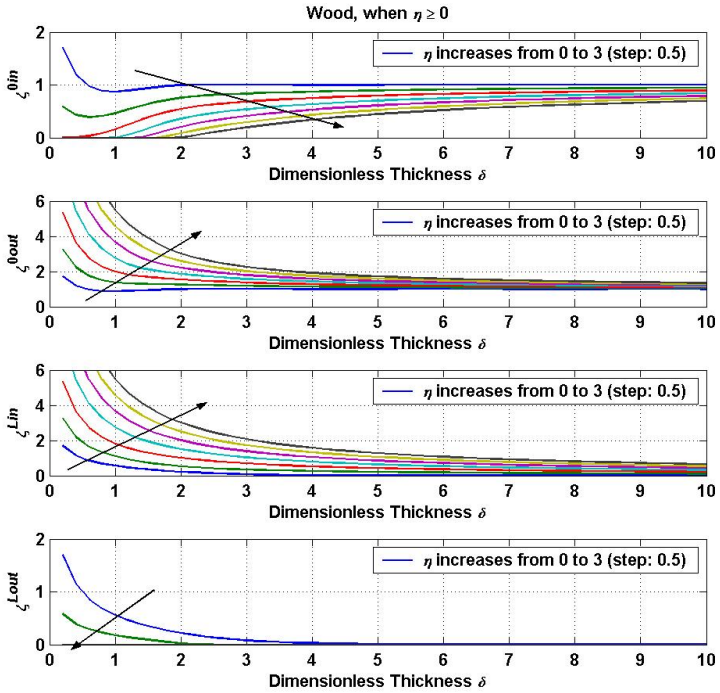

Figure 4.18—Coefficients of wood walls when $\eta \geq 0$

Comparing with Figure 4.17, when δ is the same and η is contrary, ζ^{0in} exchanges with ζ^{0out}, and ζ^{Lin} exchanges with ζ^{Lout}.

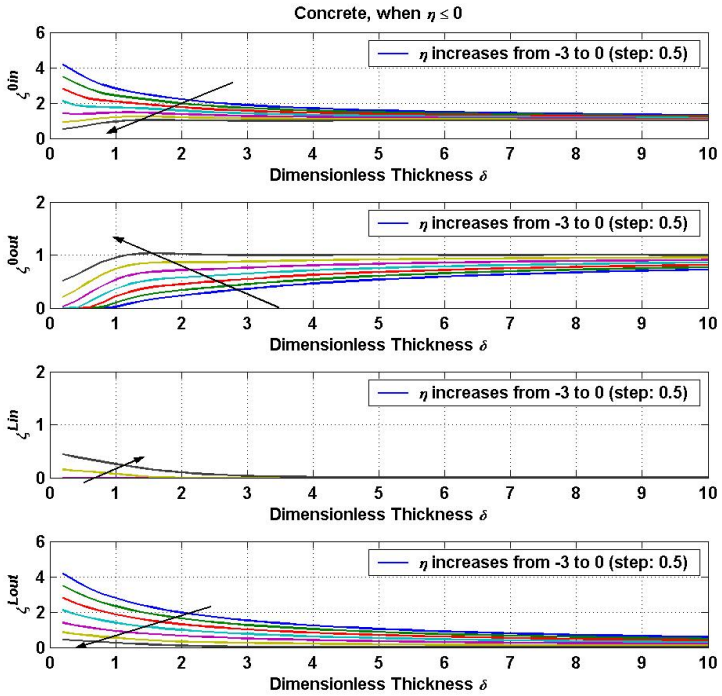

Figure 4.19—Coefficients of concrete walls when $\eta \leq 0$

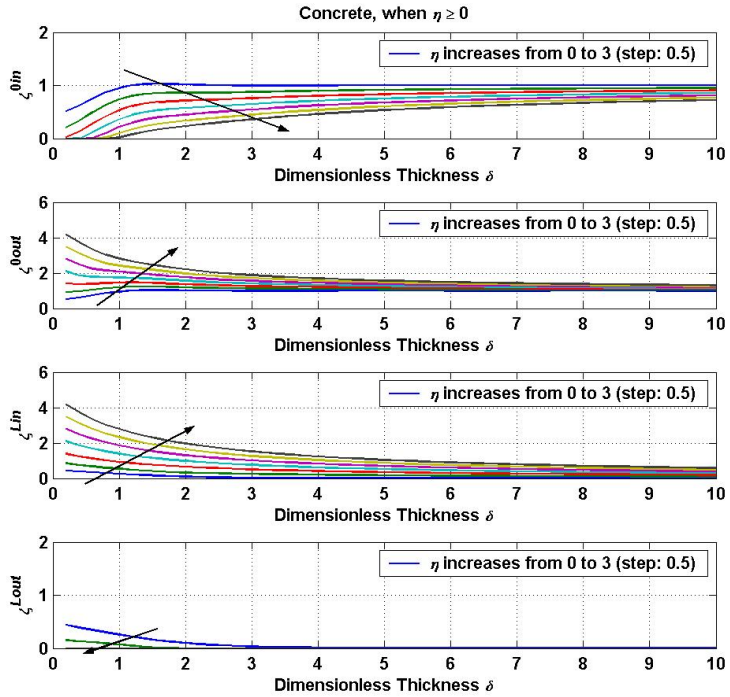

Figure 4.20—Coefficients of concrete walls when $\eta \geq 0$

Comparing Figure 4.19 and Figure 4.20 with Figure 4.17 and Figure 4.18, all corresponding coefficients of concrete walls are smaller the that of wood walls. However, this does not mean the amount of heat flowed through concrete walls is smaller than the amount of heat flowed through wood walls. That's because that when δ is the same, the thickness of a concrete wall is larger than that of a wood wall and the ratio: $\frac{c^{eff}_{area\ \text{concrete}}}{c^{eff}_{area\ \text{wood}}} = \frac{439.037}{68.207} \approx 6.437$ (Note: $\zeta \equiv \frac{Q_{max}}{Ac^{eff}_{area}\left(\Delta T\right)_0}$).

4.3.2 The time-lag effect and the decrement factor

For external PTMs, the time-lag effect and the decrement factor (see Eqn. (4. 35)) are much more important than that for internal PTMs. In this section, based on the temperature distribution of Form II, the time-lag effect and the decrement factor for

external walls will be investigated.

The definitions [8] of the time lag φ and the decrement factor f are as follows:

$$\varphi = \begin{cases} t_{Ti,\min} - t_{Te,\min} \\ t_{Ti,\max} - t_{Te,\max} \end{cases} \tag{4. 34}$$

and $$f = \frac{T_{i,\max} - T_{i,\min}}{T_{e,\max} - T_{e,\min}} \tag{4. 35}$$

where $t_{Ti,\min}$, $t_{Ti,\max}$, $t_{Te,\min}$ and $t_{Te,\max}$ are the times when the interior/exterior surface temperatures research the minimum/maximum values, respectively; and $T_{i,\min}$, $T_{i,\max}$, $T_{e,\min}$ and $T_{e,\max}$ are the minimum/maximum values of the interior/exterior surface temperatures, respectively.

When $x = 0$, the surface temperature is T_0. Therefore, $T_{e,\min} = -(\Delta T)_0$ when $t_{Te,\min} = 18\,\text{hr}$, and $T_{e,\max} = (\Delta T)_0$ when $t_{Te,\max} = 6\,\text{hr}$.

When $x = L$, A_1 and A_2 become

$$A_{1,x=L} = 2\sqrt{2}e^{\delta}\cos\left(\frac{2\pi t}{P} + \frac{\pi}{4} + \delta\right) \tag{4. 36}$$

$$A_{2,x=L} = 2\sqrt{2}e^{\delta}\sin\left(\frac{2\pi t}{P} + \frac{\pi}{4} + \delta\right) \tag{4. 37}$$

and then

$$\theta_{\text{II}}(L,t) = (\Delta T)_0 \left\{ \frac{2\sqrt{2}e^{\delta}}{B_1^2 + B_2^2}\left[B_1 \sin\left(\frac{2\pi t}{P} + \frac{\pi}{4} + \delta\right) - B_2 \cos\left(\frac{2\pi t}{P} + \frac{\pi}{4} + \delta\right)\right] + \frac{\eta}{1 + 1/\delta\varepsilon} \right\}$$

$$\Rightarrow \theta_{\text{II}}(L,t) = (\Delta T)_0 \left[\frac{2\sqrt{2}e^{\delta}}{\sqrt{B_1^2 + B_2^2}} \sin\left(\frac{2\pi t}{P} + \frac{\pi}{4} + \delta - \varphi_{\theta_{\text{II}},x=L}\right) + \frac{\eta}{1 + 1/\delta\varepsilon} \right] \tag{4. 38}$$

where $\varphi_{\theta_{\text{II}},x=L} = \arctan\frac{B_2}{B_1} \pm n\pi$ (where $n = 0,1,2,3,\ldots$) (4. 39)

For certain ε and δ, B_1 and B_2 are constant. Thus, $\theta_{\mathrm{II},x=L}$ has maximum values

$$\theta_{\mathrm{II},x=L,\max}=\left(\Delta T\right)_0\left(\frac{2\sqrt{2}e^{\delta}}{\sqrt{B_1^2+B_2^2}}+\frac{\eta}{1+1/\delta\varepsilon}\right) \tag{4. 40}$$

$$\text{when}\quad t_{\theta_{\mathrm{II},x=L,\max}}=\frac{P}{2\pi}\left(\arctan\frac{B_2}{B_1}+\frac{\pi}{4}-\delta\right)\pm\frac{nP}{2} \tag{4. 41}$$

$$\text{and}\quad \theta_{\mathrm{II},x=L}\ \text{has minimum values}\quad \theta_{\mathrm{II},x=L,\min}=\left(\Delta T\right)_0\left(-\frac{2\sqrt{2}e^{\delta}}{\sqrt{B_1^2+B_2^2}}+\frac{\eta}{1+1/\delta\varepsilon}\right) \tag{4. 42}$$

$$\text{when}\quad t_{\theta_{\mathrm{II},x=L,\min}}=\frac{P}{2\pi}\left(\arctan\frac{B_2}{B_1}+\frac{5\pi}{4}-\delta\right)\pm\frac{nP}{2} \tag{4. 43}$$

Therefore,

$$\varphi=\begin{cases}t_{Ti,\min}-t_{Te,\min}=t_{\theta_{\mathrm{II},x=L,\min}}-18\ \text{hr}=\dfrac{P}{2\pi}\left(\arctan\dfrac{B_2}{B_1}+\dfrac{5\pi}{4}-\delta\right)\pm\dfrac{nP}{2}-18\ \text{hr}\\ t_{Ti,\max}-t_{Te,\max}=t_{\theta_{\mathrm{II},x=L,\max}}-6\ \text{hr}=\dfrac{P}{2\pi}\left(\arctan\dfrac{B_2}{B_1}+\dfrac{\pi}{4}-\delta\right)\pm\dfrac{nP}{2}-6\ \text{hr}\end{cases} \tag{4. 44}$$

$$\text{and}\quad f=\frac{T_{i,\max}-T_{i,\min}}{T_{e,\max}-T_{e,\min}}=\frac{\theta_{\mathrm{II},x=L,\max}-\theta_{\mathrm{II},x=L,\min}}{\left(\Delta T\right)_0-\left[-\left(\Delta T\right)_0\right]}=\frac{2\sqrt{2}e^{\delta}}{\sqrt{B_1^2+B_2^2}} \tag{4. 45}$$

The two equations above show that φ and f are independent of η. Thus, let's change the value of ε and δ to see what will happen to φ and f. Some curves of φ and f are plotted in Figure 4.21 and Figure 4.22, respectively.

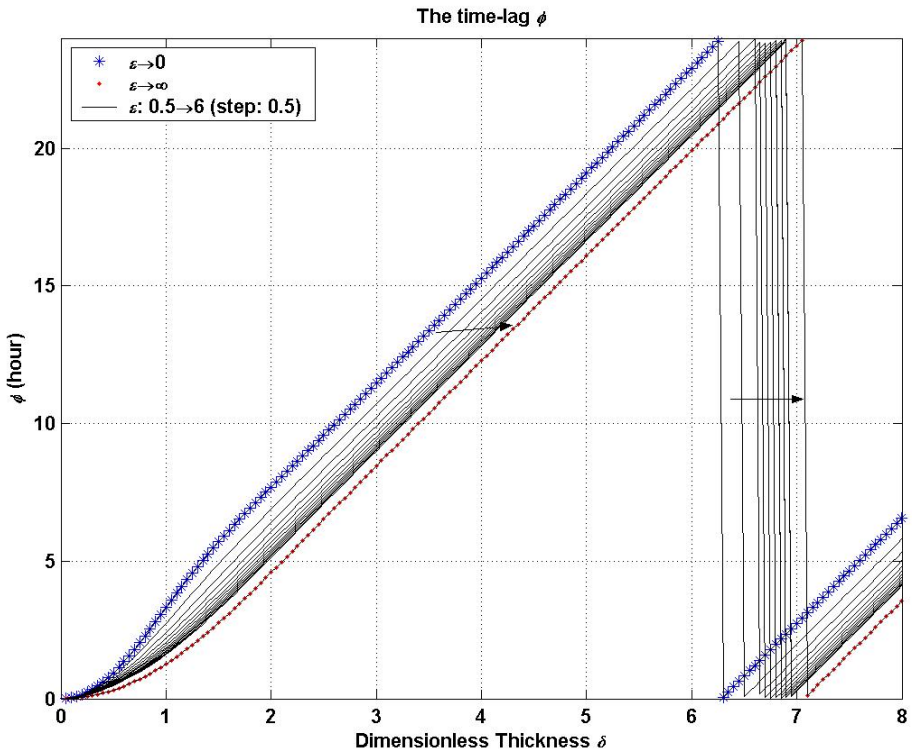

Figure 4.21—The time lag

From the figure above, we can find that

(a) When δ is smaller than about 1 and ε is the same, φ increases non-linearly as the increase of δ.

(b) When δ is the same, as ε increases from zero to positive infinity, φ decreases about 2.5 hours, except when δ is smaller than about 1;

(c) When ε is the same, as δ increases from about 1 to about 6 or 7, φ increases almost linearly to 24 hours (one period);

(d) At about 6 or 7, φ decreases from 24 hours to 0 suddenly, which means that the time lags more than one period; and the shift point decreases as ε increases;

(e) The change is very small when ε is larger than about 5.

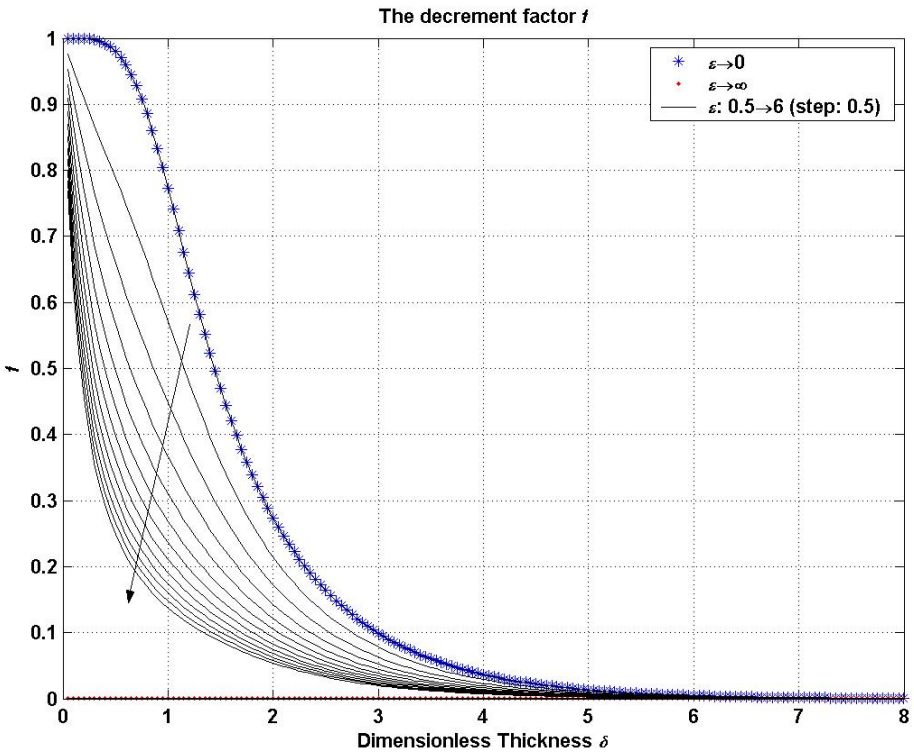

Figure 4.22—The decrement factor

In the figure above, the decrement factor is obvious non-linear. When δ is the same, as ε increases, f decreases. When ε trends to positive infinity, f is zero for all δ since both $T_{i,\max}$ and $T_{i,\min}$ are zero when the inside surface temperature keeps constant. When ε is the same, as δ increases, f decreases from nearly 1 to 0 and the decrease is very sharp when δ is small.

Again take wood and concrete walls for examples, the time lag and the decrement factor are shown in Figure 4.23, Figure 4.24, Figure 4.25, Figure 4.26, Figure 4.27 and Figure 4.28 as follows.

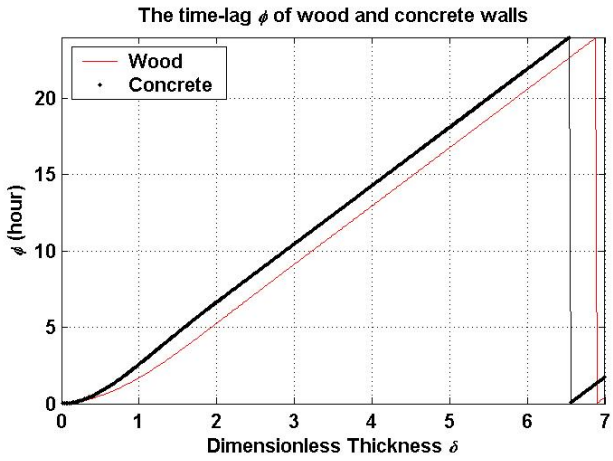

Figure 4.23—The time lag of wood/concrete walls (against δ)

In the figure above, when δ is the same, the time lag of a concrete wall is larger about 80 minutes than that of a wood wall, except when δ is smaller than about 1.

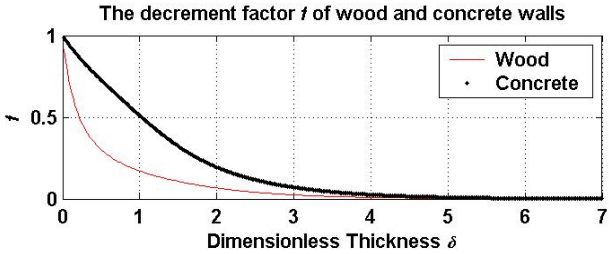

Figure 4.24—The decrement factor of wood/concrete walls (against δ)

In the figure above, the decrement factor of a wood wall is much smaller than that of a concrete wall, when δ is the same (especially when δ is smaller than about 3).

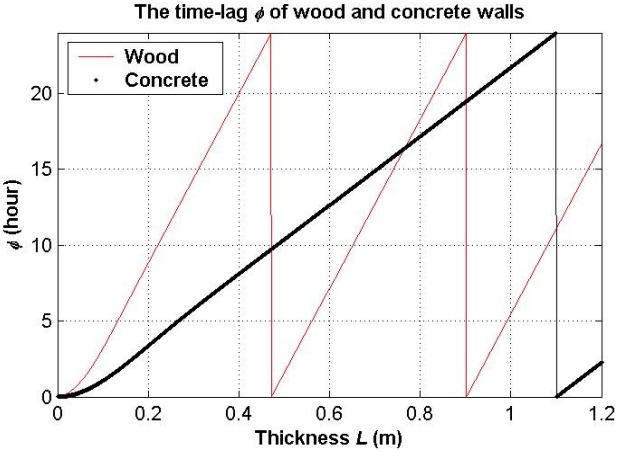

Figure 4.25—The time lag of wood/concrete walls (against L)

In the figure above, when the real thickness L is the same, the time lag of a wood wall is much larger than that of a concrete wall.

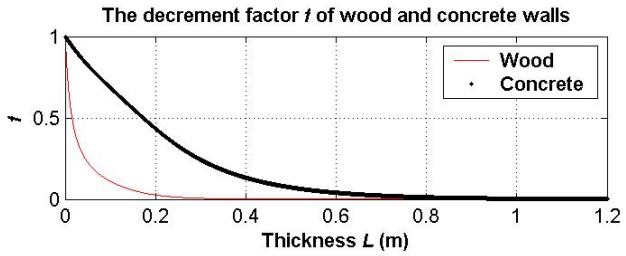

Figure 4.26—The decrement factor of wood/concrete walls (against L)

In the figure above, the decrement factor of a wood wall is much smaller than that of a concrete wall, when L is the same (especially when L is smaller than about 0.6 m).

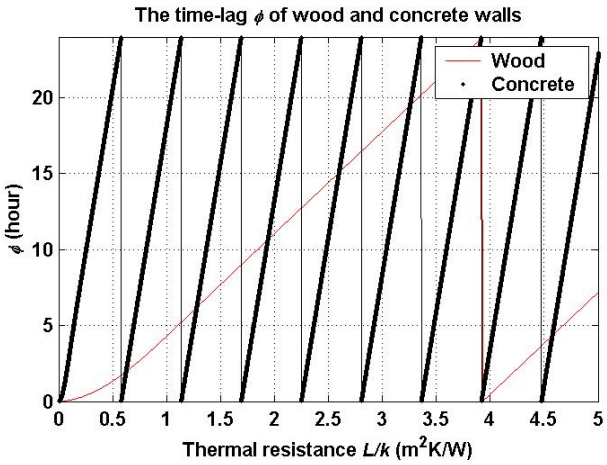

Figure 4.27—The time lag of wood/concrete walls (against L/k)

In the figure above, when the thermal resistance L/k is the same, the time lag of a concrete wall is much larger than that of a wood wall. However, the L/k value of a concrete wall cannot be too large, since when $L/k \approx 0.5$ m^{2}K/W, the real thickness of the concrete wall is already about 1m, which is too thick to be used in common buildings. Contrarily, for a typical wood wall, the corresponding L/k value can be large, since its thermal conductivity is much smaller than a concrete wall (when $L/k \approx 4$ m^{2}K/W, the

real thickness of the wood wall is just about 0.5 m).

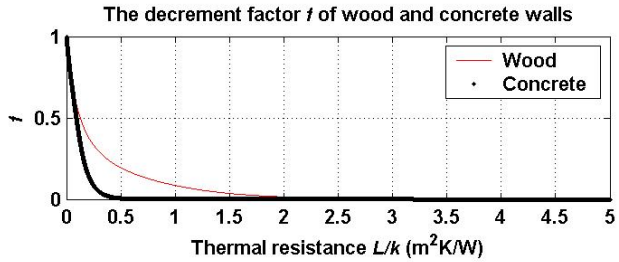

Figure 4.28—The decrement factor of wood/concrete walls (against *L/k*)

In the figure above, the decrement factor of a concrete wall is smaller than that of a wood wall, when the thermal resistance is the same (the result is not surprising since the concrete wall is about 15 times thicker than the wood wall under this condition.).

4.3.3 Correction of some rules of thumb

Some rules of thumb may need to be corrected based on the investigation above.

Rule of thumb one: "In hot and dry climates, one usually finds massive walls used for their time-lag effect." ([5]: page 3)

Compared to wood walls, concrete walls are massive. However, when the thickness is the same, the time-lag effect of a wood wall is larger than that of a concrete wall as shown in Figure 4.25. Moreover, the decrement factor of a wood wall is smaller than that of a concrete wall as shown in Figure 4.26. That is to say, for an exterior wall, a wood wall is much better than a same-thickness concrete wall, if just considering the time-lag effect and the decrement factor. Therefore, the massive walls usually used in hot and dry climates may be not because of their time-lag effect, but because of other reasons, for instance, wood is rarer in desert regions.

Rule of thumb two: On page 51 of reference [5], it explains the "insulating effect of mass". "If the temperature difference across a massive material fluctuates in certain specific ways, then the massive material will act as if it had high thermal resistance."

In fact, the "higher thermal resistance" insulating effect of mass never occurs. When $|\eta| > 1$, whether the material is massive or not, T_{out} can be treated as T_m and the amount of heat flowed into or out of the inside air is exactly equal to the steady state value, as we mentioned before (see the cases of Las Vegas and Boston, as shown in Figure 4.11, Figure 4.12, Figure 4.13 and Figure 4.14). When $|\eta| < 1$ and δ is small, walls seem to act as if it had *low* thermal resistance because of the outdoor temperature fluctuation (see the cases of Denver as shown in Figure 4.15 and 4.16; ζ^{Lin} is bigger than ζ^{steady}, which means that more heat flowed into the inside wall surface from the inside air; this greater part of heat flows back later, which is presented by ζ^{Lout}; combining ζ^{Lin} and ζ^{Lout}, the net heat flowed through the inside surface is again exactly equal to the steady state value.) Therefore, based on the investigation in this thesis, there is no such "higher thermal resistance" "insulating effect of mass".

Rule of thumb three: "Walls with high time lags and small decrement factors, give comfortable inside temperatures even if the outside is very hot". [9, 10]

In fact, this statement is not very exact. For the decrement factor, the smaller, of course, the better; but for the time lag, it is not the higher, the better. For example, a wall with a one-period time lag seems no time lag at all. A wall with a half-period time lag and a very small decrement factor is considered the best.

4.4 Summary

In this chapter, when $T_{inside\ air} \neq T_m$, the dynamic heat transfer of finite-thickness PTMs is investigated. Since analytical method is hard to be used under this condition, the finite-difference method, one of the most frequently used numerical methods, is used to solve the problem. Later, based on numerical calculation results, approximated analytical solutions are developed. Then one of the analytical solutions is used to obtain the coefficients of wood and concrete walls, the time-lag effect and the decrement factor.

Chapter 5: Conclusions and Future Work

In this thesis, the performance of PTMs subject sinusoidal heating and cooling has been investigated. Some main conclusions are summarized as follows:

1) For finite-thickness PTMs with certain ε, ζ^0 and ζ^{stor} both vary as a decaying wave with the increase of δ, and finally keep at 1;
2) After a certain thickness, thickening a PTM makes it a worse thermal mass;
3) Because of the large effective area specific heat difference, when subjected to periodic heating and cooling, a wood wall is always a poor thermal mass than a concrete wall larger than a certain thickness (2.2 cm in this thesis);
4) For a certain material, an internal PTM with the thickness of $L = 2L^* \approx 0.5323L_{pene} \approx 1.6723L^{eff}$ is the best thermal mass;
5) For certain ε and δ, ζ^{stor} is the same, no matter $T_{inside\ air} = T_m$ or not;
6) If δ is not too small, T_{out} can be treated as T_m and the total heat flowed into the inside air just depends on the wall thermal resistance;
7) The time lag and the decrement factor are both independent of the environment temperature;
8) For exterior walls, a wood wall is much better than a same-thickness concrete wall, if just considering the time-lag effect and the decrement factor;
9) The time lag is not the higher, the better;

10) The higher thermal resistance insulating effect of mass does not exist.

Some suggestions of future work are listed as follows:

1) Since most walls are multilayered, dynamic heat transfer of multilayer PTMs should be investigated;
2) Dynamic heat transfer should be investigated when material thermo-physical properties are not constant;
3) A dynamic heat transfer model should be built by combining building envelop, internal thermal masses and the environment.

Reference

[1] Chris Reardon. *Your home: design for lifestyle and the future. technical manual* 4th edition, 2008

[2] B. Haglund, K. Rathmann. *Thermal mass in passive solar and energy-conserving buildings*. 1995

[3] K. Gregory, B. Moghtaderi, H. Sugo, A. Page. *Effect of thermal mass on the thermal performance of various Australian residential constructions systems*. Energy and Buildings 40 (2008) p.459-465

[4] G. Z. Brown, Mark DeKay. *Sun, Wind & Light: Architectural Design Strategies* 2nd Edition. John Wiley & Sons, 2000.10

[5] Norbert Lechner. *Heating, Cooling, Lighting: Sustainable Design Methods for Architects* 3rd edition. John Wiley & Sons, 2008

[6] K. W. Childs, G. E. Courville, E. L. Bales. ***Thermal Mass Assessment****—An Explanation of the Mechanisms by Which Building Mass Influences Heating and Cooling Energy Requirement.* 1983.9

[7] K. R. Keeney, J. E. Braun. *Application of building precooling to reduce peak cooling requirements*. ASHRAE transactions (1997) p.463

[8] K.J. Kontoleon, D.K. Bikas. *Thermal mass vs. thermal response factors: determining optimal geometrical properties and envelope assemblies of building materials*. International Conference “Passive and Low Energy Cooling for the Built Environment”, May 2005, Santorini, Greece

[9] H. Asan, Y.S. Sancaktar. *Effects of Wall’s thermophysical properties on time lag and decrement factor*. Energy and Buildings 28 (1998) 159-166

[10] T.R. Knowles. *Proportioning composites for efficient thermal storage walls*. Solar Energy 31 (3) (1983) 319-326

[11] S. Ferrari. *Building envelope and heat capacity: re-discovering the thermal mass for winter energy saving*. 2nd PALENC Conference and 28th AIVC Conference on Building Low Energy Cooling and Advanced Ventilation Technologies in the 21st Century, September 2007, Crete island, Greece

[12] L. Yang, Y. Li. *Cooling load reduction by using thermal mass and night ventilation*. Energy and Buildings 40 (2008) 2052−2058

[13] J. Zhou, G. Zhang, Y. Lin, Y. Li. *Coupling of thermal mass and natural ventilation in*

buildings. Energy and Buildings 40 (2008) 979–986

[14] L. Zhu, R. Hurt, D. Correia, R. Boehm. *Detailed energy saving performance analyses on thermal mass walls demonstrated in a zero energy house*. Energy and Buildings 41 (2009) 303−310

[15] V. Cheng, E. Ng, B. Givoni. *Effect of envelope colour and thermal mass on indoor temperatures in hot humid climate*. Solar Energy 78 (2005) 528−534

[16] K. Gregory, B. Moghtaderi, H. Sugo, A. Page. *Effect of thermal mass on the thermal performance of various Australian residential constructions systems*. Energy and Buildings 40 (2008) 459–465

[17] B. Givoni. *Effectiveness of mass and night ventilation in lowering the indoor daytime temperatures. Part I: 1993 experimental periods*. Energy and Buildings 28 (1998) 25-32

[18] P. L. Roche, M. Milne. *Effects of window size and thermal mass on building comfort using an intelligent ventilation controller*. Solar Energy 77 (2004) 421–434

[19] J. N. Hacker, T. P. De Saulles, A. J. Minson, M. J. Holmes. *Embodied and operational carbon dioxide emissions from housing: A case study on the effects of thermal mass and climate change*. Energy and Buildings 40 (2008) 375–384

[20] S. A. Kalogirou, G. Florides, S. Tassou. *Energy analysis of buildings employing thermal mass in Cyprus*. Renewable Energy 27 (2002) 353–368

[21] Baharuddin. *Energy efficient commercial building design strategies*. RONA Jurnal Arsitektur FT-Unhas Volume 2 No. 1, April 2005, hal. 1-18

[22] J. E. Braun, K. W. Montgomery, N. Chaturvedi. *Evaluating the Performance of Building Thermal Mass Control Strategies*. HVAC&R RESEARCH Vol. 7, No. 4. October 2001

[23] G. P. Henze, J. Pfafferott, S. Herkel, C. Felsmann. Impact of adaptive comfort criteria and heat waves on optimal building thermal mass control. Energy and Buildings 39 (2007) 221–235

[24] J. E. Braun. *Load Control Using Building Thermal Mass*. Journal of Solar Energy Engineering Vol. 125 p.292-301 August 2003

[25] K. Lee, J. E. Braun. *Model-based demand-limiting control of building thermal mass*. Building and Environment 43 (2008) 1633-1646

[26] J. Yam, Y. Li, Z. Zheng. *Nonlinear coupling between thermal mass and natural ventilation in buildings*. International Journal of Heat and Mass Transfer 46 (2003) 1251-1264

[27] M. J. Brown. *Optimization of Thermal Mass in Commercial Building Applications*. Journal of Solar Energy Engineering Vol. 112 p.273-279 November 1990

[28] S. Wang, X. Xu. *Parameter estimation of internal thermal mass of building dynamic models using genetic algorithm*. Energy Conversion and Management 47 (2006) 1927-1941

[29] D. M. Ogoli. *Predicting indoor temperatures in closed buildings with high thermal mass*. Energy and Buildings 35 (2003) 851–862

[30] T. Y. Chen. *Real-time predictive supervisory operation of building thermal systems with thermal mass*. Energy and Buildings 33 (2001) 141-150

[31] C.A. Balaras. *The role of thermal mass on the cooling load of buildings. An overview of computational methods*. Energy and Buildings 24 (1996) l-10

[32] S. P. Corgnati, A. Kindinis. *Thermal mass activation by hollow core slab coupled with night ventilation to reduce summer cooling loads*. Building and Environment 42 (2007) 3285−3297

[33] E. Shaviv, A. Yezioro, I. G. Capeluto. *Thermal mass and night ventilation as passive cooling design strategy*. Renewable Energy 24 (2001) 445–452

[34] G. Y. Yun, P. Tuohy, K. Steemers. *Thermal performance of a naturally ventilated building using a combined algorithm of probabilistic occupant behaviour and deterministic heat and mass balance models*. Energy and Buildings 41 (2009) 489-499

[34] S. Kakaç, Y. Yener. *Heat Conduction* 3rd edition. Taylor & Francis, 1993